Salivary proteins of *Phloeomyzus passerinii*, a plant-manipulating aphid, and their impact on early gene responses of susceptible and resistant poplar genotypes

Luis Portillo Lemus [1, 2] *, Jessy Tricard [1, 2] *, Jérôme Duclercq [2], Quentin Coulette [2], David Giron [3], Christophe Hano [1], Elisabeth Huguet [3], Frédéric Lamblin [1], Anas Cherqui [2] °, Aurélien Sallé [1] °†

[1] Laboratoire de Biologie des Ligneux et des Grandes Cultures, INRA, Université d'Orléans, 45067, Orléans, France

[2] Ecologie et Dynamique des Systèmes Anthropisés, EDYSAN UMR CNRS-UPJV 7058, Université de Picardie Jules Verne, Amiens, France

[3] Institut de Recherche sur la Biologie de l'Insecte, UMR 7261, CNRS/Université François-Rabelais de Tours, Tours, France

* L. Portillo Lemus and J. Tricard should be considered joint first author

° A. Cherqui and A. Sallé should be considered joint senior author

† corresponding author

Declarations of interest: none

Authors' contribution

- AC, AS and DG conceived the ideas. JD, AC and AS designed methodology. LPL, JD and FL collected the plant-related data. JT, QC, CH and EH collected the insect-related data. LPL and JT analyzed the data. AC and AS led the writing of the manuscript. All authors have read and approved the manuscript.

Abstract

Plant manipulation by herbivores requires fine-tuned reprogramming of host metabolism, mediated by effector molecules delivered by the parasite into its host. However, secretomes of plant-manipulating animals and their impact on host-plants have been rarely studied. Using transcriptomic and enzymatic approaches, we characterized salivary glands and saliva of a plant-manipulating aphid, *Phloeomyzus passerinii*. Plant genes responses to aphid saliva were assessed *in vivo*, with poplar protoplasts of a susceptible and a resistant genotype, and *in planta* in a heterologous *Arabidopsis* system. Responses to salivary extracts of *P. passerinii* were compared to those of *Myzus persicae*, a sap-feeder which does not feed on poplars. Effectors potentially interfering with plant signaling have been identified in the salivary glands, including binding proteins, oxidoreductases, and phosphatidylinositol phosphate kinases. Gene expression profiles markedly differed between aphid species, and according to plant genotype for protoplasts exposed to the saliva of *P. passerinii*. Compatible interactions between *P. passerinii* and the susceptible poplar genotype affected cytokinin signalization and auxin homeostasis, potentially leading to an intracellular accumulation of auxin, which was further supported by *in planta* assays, and triggering a change in developmental cell fate. The overall response to *P. passerinii* during compatible interactions suggests congruent manipulation mechanisms with gall-inducing nematodes.

Keywords

Effector, *Myzus persicae*, *Phloeomyzus passerinii*, plant-insect interaction, *Populus*, resistance

45 **1 Introduction**

46

47 Nutritional imbalance and defense mechanisms are major hurdles hampering plant resources
48 exploitation by animals [1]. To cope with this, some herbivores have evolved strategies consisting in
49 remodeling plant tissues to turn them into optimal substrates for their development and fitness [2], with
50 sometimes spectacular and complex tissue reorganization resulting in new plant organs, within which
51 parasites feed and grow [3, 4, 5]. To adapt plant tissues to nutritional requirements of parasites and to
52 circumvent plant defenses, manipulation implies fine-tuned metabolism reprogramming, and direct
53 modulations of both primary and secondary metabolisms of host plants have been reported for plant-
54 manipulating organisms [5]. More specifically, since they are important regulators of plant growth,
55 differentiation and defense, phytohormones are classical targets of plant-manipulating organisms, and
56 considered key factors intimately involved in the success or failure of manipulation [5, 6].
57 Host metabolism hijacking by plant-manipulating organisms is considered to be mediated by effector
58 molecules delivered into the host-plant [5, 7]. Effector proteins secreted by herbivores in general have
59 various functions, including suppression of plant defense, alteration of plant development, and
60 manipulation of plant resources [5, 7]. For plant-manipulating organisms, similar functions are expected,
61 especially disruption or diversion of hormone-dependent pathways [6] and inactivation of second
62 messengers involved in stress signaling like Ca^{2+}, reactive oxygen species (ROS) and extracellular ATP for
63 instance [8, 9]. While there is a growing literature dealing with the identification of these effectors in
64 herbivores, like aphids [e.g. 10, 11, 12, 13], few investigations have been performed on secretions of
65 plant-manipulating animals, with notable exceptions of the Hessian fly (*Mayetiola destructor* (Say)) and
66 root-knot nematodes (*Meloidogyne* spp.) for instance [e.g. 14, 15]. So far, the Hessian fly is the only
67 member of plant-manipulating insects with a sequenced genome, and whose salivary gland
68 transcriptome and proteome have been studied [14, 16]. Candidate genes with effector functions have

69 been detected and gene-for-gene interaction between insect strains and host-plant genotypes has been
70 demonstrated [14, 16, 17]. How these effectors contribute to manipulation is still unclear, but it is
71 hypothesized that they interfere with downstream signaling and phytohormone pathways [5].
72 To validate the relevance of candidate effectors for plant-insect interactions, several approaches have
73 been used. *In planta* modulation of candidate effectors expression allowed to highlight impacts of
74 effector proteins on physiological traits and behavior of insects and plant responses [e.g. 17, 18, 19].
75 Alternatively, direct applications of oral secretions and saliva infiltration into host plants also gave
76 conclusive results [e.g. 20, 21]. Nonetheless, probably because of their complex life cycles and often
77 concealed endophytic development, very few functional validation experiments have been performed
78 with plant-manipulating insects [e.g. 17]. In-depth functional molecular approaches would allow to
79 unravel the mechanisms that contribute to plant manipulation by these organisms and could possibly
80 lead to identification of convergent mechanisms among them [5].
81 Here, we report the characterization of salivary proteins of *Phloeomyzus passerinii* Sign., a plant-
82 manipulating aphid colonizing poplars [22]. This aphid feeds on cell contents in the cortical parenchyma
83 of its host-trees [22, 23, 24]. In susceptible hosts, aphid probing triggers cell multiplication in cortical
84 parenchyma and, later, thin-walled hypertrophied cells differentiate while starch and vacuolar phenolic
85 compounds disappear, and amino acids accumulate [24, 25]. Consequently, infestations by *P. passerinii*
86 induced peculiar anatomical and biochemical modifications in host tissues, different from those
87 observed following mechanical injuries [24]. In addition, further experiments also showed that insect
88 performance was enhanced and feeding behavior was optimized on manipulated cortical tissues [26]. It
89 is therefore considered that *P. passerinii* manipulates the cortical parenchyma of its susceptible hosts,
90 and induces a pseudogall, i.e. a swelling of preexisting plant tissues, to improve the nutritional value of
91 its host tissues [22, 24]. In resistant host genotypes, lignin, tannins and flavanols accumulate at the
92 probing site one week after the onset of probing and no pseudogall differentiation occurs subsequently

93 [24]. As a consequence, *P. passerinii* cannot develop on these genotypes [24].

94

95 As this insect can be easily handled under laboratory conditions, and its saliva can be collected on
96 artificial medium, we performed innovative functional validation assays to address the impact of the
97 saliva of a plant-manipulating organism on gene responses of its host-plant. Our objectives were (i) to
98 characterize with transcriptomic and enzymatic approaches the salivary glands and saliva, respectively,
99 of *P. passerinii*, (ii) to assess *in vivo*, with a RT-qPCR approach, early responses of poplar genes belonging
100 to different metabolic and signaling pathways using protoplasts exposed to aphid saliva, and (iii) to
101 investigate the impact of salivary extracts on specific gene expression *in planta*, in a heterologous
102 *Arabidopsis* system. For all these steps comparative approaches have been used. The determined
103 salivary proteins of *P. passerinii* were compared with those of a sap-feeding aphid, *Myzus persicae*
104 (Sulzer) [10, 20], in order to identify proteins common to both aphid species as well as proteins specific
105 to *P. passerinii*. To get insight into how *P. passerinii* affects host metabolism and stress responses to
106 perform manipulation, the impact of salivary extracts on gene expression has been assessed with poplar
107 genotypes either susceptible or resistant to *P. passerinii*, i.e. during compatible and incompatible
108 interactions, respectively. These poplar genotypes have also been exposed to salivary extracts of *M.*
109 *persicae*, which led to non-host interactions since *M. persicae* does not feed on poplar.

110

111 ## 2 Materials and Methods

112

113 ### 2.1 Plant and insect material

114 All individuals of *P. passerinii* used either for transcriptomic analyses of salivary glands or saliva collection
115 originated from the same monoclonal colony established from an apterous parthenogenetic female,
116 collected in 2013 in Brézé (France, 47°16'36'' N 0°06'84'' W, WGS-84). The colony was maintained in the
117 laboratory on potted stem cuttings of I-214, a *Populus x canadensis* Moench. genotype, under 20 ± 1 °C,
118 70 ± 10% relative humidity and 16/8 h light/dark cycles. The green peach aphid, *M. persicae* is a sap-
119 feeder. Both *P. passerinii* and *M. persicae* are Aphididae, but belong to different subfamilies (*P. passerinii*
120 is the only member of the Phloeomyzinae while *M. persicae* is an Aphidinae), which diverged at 137 Ma
121 [27]. *Myzus persicae* is a generalist aphid but its host range does not include poplars, and preliminary
122 establishment attempts confirmed that it cannot settle and develop on poplars (data not shown).
123 Therefore non-host interactions are expected between this aphid species and poplar genotypes.
124 Individuals of *M. persicae* originated from a monoclonal colony established from an apterous
125 parthenogenetic female collected in 1999 on a potato plant in Loos-en-Gohelle (France, 50°27'44" N
126 2°46'45" E, WGS-84). The colony was maintained under the same controlled conditions as *P. passerinii*,
127 on turnips (Vilmorin).
128
129 For the protoplasts production, stem-cuttings of two *P. x canadensis* genotypes commonly planted in
130 France, I-214 and Koster, were used for the experiments. I-214 is highly susceptible to *P. passerinii*,
131 whereas aphids cannot settle on Koster which is consequently considered to be highly resistant to *P.*
132 *passerinii* [22]. Consequently, compatible and incompatible interactions are expected between *P.*
133 *passerinii* and I-214 and Koster, respectively, and non-host interactions should take place between *M.*
134 *persicae* and both poplar genotypes. Stem cuttings (ca. 25 cm long, 2 cm diameter) were provided by the
135 experimental nursery of Guéméné-Penfao (Office National des Forêts, France). They were collected in
136 the autumn of 2016, and kept at 2°C, in dry conditions until use. In January 2017, the stem-cuttings were
137 removed from storage and planted in 0.4 L pots, filled with a sterile sand-compost (50:50) mixture

138 (Klasmann substrate 4 no. 267). The cuttings were then transferred to a growth chamber (20 ± 1°C, 70 ±
139 10% relative humidity, 16/8 h light/dark photoperiod, 2.65 kLx, and watered three times a week).
140 For *in planta* functional validation of the effects of salivary proteins, two transgenic lines of *Arabidopsis*
141 *thaliana* (L.) Heynh. were used. The transgenic line *pIAA2*::GUS [28] was used to assess the auxin
142 response, with its auxin-responsive promoter, while the cytokinin response was evaluated with
143 *pARR16*::GUS, with its cytokinin-responsive promoter [29].
144
145 Seeds were sterilized with chloral gas, sown in Petri dishes on 0.8% (w/v) agar with 1% (w/v) sucrose-
146 containing 0.5 Murashige and Skoog medium (MS), stored for 2 days at 4°C, and grown on vertically
147 oriented plates in growth chambers under a 16/8 h light/dark photoperiod at 18°C.
148
149 **2.2 Salivary transcriptome**
150
151 **2.2.1 Sample collection, RNA isolation and *de novo* transcriptome assembly**
152 About 500 adults of apterous parthenogenetic *P. passerinii* aphids, collected directly on their host-plant,
153 were dissected to collect pairs of salivary glands. Total RNA was extracted using the GeneJET RNA
154 Purification kit (Thermo Fischer Scientific), according to manufacturer's instructions. RNA was DNase
155 treated using RNase-Free DNase Set (Qiagen). RNA concentration was measured using the Qubit® RNA
156 Assay Kit (Life Technologies) and a Qubit® 2.0 Fluorometer (Invitrogen). Construction of cDNA-library and
157 sequencing were performed by Eurofins® Genomics using a MiSeq v3 Reagent Kit (600 Cycles PE,
158 Illumina, USA) and a MiSeq sequencer (Illumina), with 12.5 µg of total RNA. For the *de novo*
159 transcriptome assembly, 15,453,942 pair-ended reads were sequenced and assembled using Velvet
160 (v1.2.10; [30]) and Oases (v0.2.8; [31]) software tools (table S1). A multi-kmer approach was applied.
161 Separate assemblies with different kmer lengths have been conducted and the individual assemblies

162 have been merged to a final assembly. Kmer lengths of 69, 89, 109 and 129 were used. The separate
163 assemblies were merged following the filter1-CD-HIT-EST procedure proposed in Yang & Smith [32]. A
164 completeness assessment was performed using gVolante (v1.2.1; [33]) with the pipeline BUSCO v2/v3
165 and the reference dataset Arthropoda (table S1). This Transcriptome Shotgun Assembly project has been
166 deposited at DDBJ/EMBL/GenBank under the accession GHDF00000000. The version described in this
167 paper is the first version, GHDF01000000.
168

169 **2.2.2 Annotation, secreted proteins detection and identification**

170 To perform comparisons with *M. persicae* the transcriptome of this aphid was retrieved on NCBI
171 (http://www.ncbi.nlm.nih.gov/genbank/, accession numbers: DW010205 - DW015017, EC387039 -
172 EC390992, EE570018 - EE572264, EE260858 - EE265165, ES444641 - ES444705, ES217505 - ES226848,
173 and ES449829 - ES451794). Salivary transcriptomes have been annotated using the pipeline described in
174 figure S1. Transcripts were first translated into amino acid sequences using Prodigal (v2.5; [34]). We then
175 used the SignalP 4.0 Server (v4.1) to predict the presence of signal peptides and cleavage sites in the
176 amino acid sequences [35]. To predict transmembrane domains, we submitted each amino acid
177 sequence with a signal peptide to the TMHMM Server (v. 2.0; [36]). Putative proteins with a signal
178 peptide and no transmembrane domain were considered to be potential secreted proteins. The
179 sequences of complete ORFs without signal peptide were analyzed again with SecretomeP (v2.0; [37]).
180 To remove mitochondrial proteins with a signal peptide, which are not secreted in the saliva, sequences
181 were analyzed with TargetP (v1.1; [38]). Likewise, to remove proteins of the endoplasmic reticulum with
182 a signal peptide, sequences were analyzed with PS-scan (Prosite pattern: PS00014), and with PredGPI
183 [39] for glycosylphosphatidylinositol-anchor signals.
184 The remaining proteins were first mapped against the non-redundant protein sequences (nr) using
185 Blastp (v2.3.0, NCBI, accessed on 03/30/2016), with an E-value cutoff at 1^{e-3}. Protein domains were

186 annotated with Blast2Go (v3.3; [40]), and InterProScan (v5.30-69; [41]). Whenever possible, protein
187 sequences were assigned to Gene ontology (GO) terms with an E-value cutoff at 1^{e-6}, enzyme codes (EC)
188 and KEGG pathways.
189 OrthoVenn (http://aegilops.wheat.ucdavis.edu/OrthoVenn; [42]) has been used to identify orthologous
190 proteins within and between salivary transcriptomes of the two aphids. Intraspecific orthologous
191 proteins are first grouped into clusters, which are then compared between species. Each cluster has
192 been annotated with the Uniprot database (http://www.uniprot.org; [43]) and the nr peptide sequence
193 database (NCBI, accessed on 03/30/2016).
194 To detect proteins orthologous to salivary effectors of aphids, protein sequences of known aphid
195 effectors, i.e. C002, ACE1, ACE2, ACYPI39568, ACYPI00346, MpC002, Mp1, Mp2, Mp42, Mp55, Me10,
196 Me23 [44, 45, 46], have been compared to the salivary transcriptome of *P. passerinii* with Blastp (E-value
197 $\leq 1^{e-3}$).
198
199 **2.3 Functional validation assays**
200
201 **2.3.1 Aphid saliva collection**
202 Aphids secrete two types of saliva within their host-plants, liquid and solid saliva [8]. The solid saliva is
203 secreted during probing. It hardens rapidly and forms a solid sheath encasing aphid stylets within the
204 host-plant, while the liquid saliva is secreted within cells and sieve tubes [8]. Both types of saliva contain
205 effectors [e.g. 8, 47], and have been collected in our experiments. Because of the particular trophic
206 substrates of *M. persicae* and *P. passerinii* (i.e. sap and galled tissues, respectively), a special protocol has
207 been used for each species. The saliva of *P. passerinii* was collected after incubation of 30 to 40
208 individuals of 2nd and 3rd instars aphids on sachets of Parafilm© membranes containing an artificial diet
209 [48]. The artificial diets were constituted by a disc of 0.5% (w/v) agar completed with 150 µL of 15%

210 (w/v) sucrose. The saliva of *M. persicae* was collected after incubation of 30 to 40 individuals, of 3rd and
211 4th instars, on artificial diet containing 120 µL of a 15% (w/v) sucrose as previously described by Cherqui
212 & Tjallingii [48]. Aphids were deposited in a feeding chamber during 24 h at 20°C, 60 ± 1% relative
213 humidity and a 16/8 h light/dark period with 2.65 kLx. Feeding chambers containing the artificial diets,
214 incubated in the absence of aphids, were used as control samples.
215 For *P. passerinii*, after 24 h aphid salivation, artificial diet discs were collected and transferred into 100
216 µL of TE buffer (10 mM Tris, 1 mM EDTA, pH 8). The salivary proteins were released from the artificial
217 diet according to Yang et al. [49], with slight modifications. The tubes containing artificial diet discs were
218 frozen in liquid nitrogen for 1 min, immediately thawed at 70°C for 3 min and then centrifuged at 11,000
219 x *g* for 20 sec. To discard the excess of agar, salivary extracts were centrifuged in Sartorius tubes with
220 filters of 0.22 µm. The supernatant containing salivary proteins of *P. passerinii* were collected, pooled
221 and then stored at -20°C. For *M. persicae,* after 24 h salivation, aphid saliva was collected according to
222 Harmel et al. [10]. The artificial diet is collected containing soluble saliva. The solid saliva was collected
223 during the rinsing of each lower Parafilm membrane with TE buffer containing 0.1% (w/v) of Tween 20
224 (TE/Tween). The extracts were centrifuged at 10,000 x *g* for 15 min. The salivary proteins in the pellet
225 were collected, pooled with the soluble saliva and then stored at -20°C.
226 The sample containing protein saliva extracts were concentrated using 2 mL Vivaspin© tube (Sartorius)
227 with 3kDa cut-off. The tubes were then centrifuged at 5,000 x *g* for 70 to 120 min according to sample
228 volumes, and proteins adhering to membranes were recovered by 100 µL of TE/Tween buffer. Control
229 samples were prepared with artificial diets from feeding chambers without aphids. The protein
230 quantification was performed by measuring absorbance at 280 nm with the NanoDrop© 1000
231 (ThermoScientific).
232
233 **2.3.2 Enzyme activities**

234 Several enzyme substrates were added to the previously described artificial diets with or without
235 agarose to detect enzymatic activities present in saliva excreted from the aphid. To visualize proteins in
236 the salivary sheaths, the lower Parafilm© membranes were stained by adding a drop of 0.01% (w/v)
237 Coomassie blue in 10% (v/v) glycerol for 2 h. Dihydroxyphenylalanine (DOPA), 0.1% (w/v) was added to
238 identify phenoloxidase activity (PO; catechol oxidase, EC 1.10.3.1). The enzymatic product, melanin,
239 should stain salivary sheaths and halos around the sheaths. To detect peroxidase (EC 1.11.1.7) activity,
240 artificial diets were immersed for some minutes in 0.1% (w/v) diaminobenzidine (DAB, Sigma) in 50 mM
241 Tris (pH 7.5) containing 0.1% (v/v) H_2O_2 (Sigma). The enzymatic product should induce reddish staining of
242 salivary sheaths and halos. For identification of pectinase activity, 0.1% (w/v) of pectin (Sigma) was
243 added to the medium. After exposure to aphids, the gel was transferred for 3 h into a Petri dish
244 containing 50 mM citrate-phosphate buffer, at pH 5.0 to detect pectin (methyl) esterase (PME, EC
245 3.1.1.11) and at pH 6.4 to detect polygalacturonase (PG, EC 3.1.1.15). The gel was then stained with a
246 solution of 0.01% (w/v) ruthenium red (Sigma) for 1 h, and then washed several times with distilled
247 water. At pH 6.4, red halos around the salivary sheaths indicate PME activity, while non-staining halos at
248 pH 5 in the pink pectin indicate PG activity. Finally, for proteinase activity (EC 3.4.99), 0.5% (w/v) of
249 gelatin (Sigma) was added to the medium. After exposure to aphids, the medium was incubated
250 overnight in a solution of 50 mM Tris (pH 8) containing 100 mM NaCl and 10 mM $CaCl_2$, then stained with
251 Coomassie blue. An absence of blue staining shows proteinase activity. All observations of proteins and
252 enzymatic activities were performed by light microscopy (Axioplan 2, Zeiss, Jena, Germany).
253

254 **2.3.3 Poplar protoplast preparations and treatments**

255 We wanted to assess early poplar gene responses to aphid saliva, as interactions between elicitors and
256 effectors of herbivores and plant receptors occur readily after the onset of probing or feeding [50]. Once
257 deposited on their plant material, adults and nymphs of *P. passerinii* can wait for several hours before

258 probing and delivering saliva into host tissues, inject probably a varying amount of saliva and presumably
259 affect a limited number of host cells [22, 26]. Therefore, we used protoplasts as plant material in order
260 to (i) have a sufficient amount of plant material exposed to treatments for the RT-qPCR experiments and
261 (ii) have an identical exposure duration and intensity to salivary extracts among biological replicates. This
262 also allowed to compare the effects of saliva alone from different aphid species on gene expression, *P.*
263 *passerinii* having a quite unique feeding behavior compared to other aphid species [23]. Mesophyll
264 protoplasts of the two poplar genotypes were obtained from young leaves as described in Wu et al. [51].
265 Leaves were cut into 1–2 mm fine strips in 0.3 M sorbitol and 66.67 mM $CaCl_2$ (pH 5.6) and lysed in an
266 enzyme solution (0.6 M mannitol, 0.25% (w/v) cellulase Onozuka R-10, 0.05% (w/v) macerozyme R-10) in
267 the dark for 16 h with gentle shaking (30 rpm) at room temperature. Protoplasts were collected by
268 filtering the lysate suspension through a 70 µm cell strainer (Falcon®) and concentrated by spinning
269 down at ≈ 800 x *g* for 10 min at 4 °C. The pellet was washed twice with W5 buffer (154 mM NaCl, 125
270 mM $CaCl_2$, 5 mM KCl, 5 mM glucose, 0.03% (w/v) MES, pH 5.8) and then resuspended in 0.6 M mannitol
271 to a final concentration of 1×10^6 protoplasts per mL. Protoplasts (1.10^6) were incubated at 20°C with
272 gentle shaking (40 rpm) for 3 h with aphid salivary proteins or with protein extraction buffer (control).
273 RNA extraction was done just after the saliva or control treatment (see 2.3.4). Preliminary experiments
274 investigating expression of 5 poplar genes, and conducted with 1, 10, 20, 40 or 80 µg of salivary proteins,
275 indicated that the optimal response (i.e. the maximum fold change) was observed with 1 µg of salivary
276 proteins of *P. passerinii* and that responses with a similar magnitude were observed with 10 µg of
277 salivary proteins of *M. persicae* (Fig. S2). Protoplast viability, before and after treatment with aphid
278 saliva, was assessed using 0.005% (w/v) fluorescein diacetate (FDA). After 5 min of incubation
279 protoplasts were observed under blue light epifluorescence, and cell viability was estimated as the
280 percentage of fluorescent cells. Most protoplasts were intact and viable after enzymatic digestion with
281 cellulase and macerozyme (98%), as well as after incubation with salivary proteins (95%; Fig. S3).

282

283 **2.3.4 Quantitative RT-PCR**

284 After the aphid saliva treatments, protoplasts were centrifuged at ≈ 800 x *g* for 2 min. Total RNAs were
285 then immediately extracted with the RNeasy® Plant Kit Mini Kit (Qiagen). A DNase treatment with the
286 RNase-free DNase Set (Qiagen) was carried out for 15 min at 25°C. Total RNA concentration was
287 determined using a Nanodrop ND-1000 spectrophotometer. All RNA samples were rejected if they did
288 not reach a minimum concentration of 100 ng μL^{-1}, a 260 nm/280 nm ratio between 1.8 and 2.0. Poly(dT)
289 cDNA was prepared from 1 µg total RNA using the iScriptTMcDNA Synthesis Kit (Bio-Rad) and quantified
290 with a LightCycler 480 (Roche) and SYBR GREEN I Master (Roche), according to the manufacturer's
291 instructions. PCR was carried out in 384-well optical reaction plates heated for 10 min to 95°C to activate
292 hot start Taq DNA polymerase, followed by 40 cycles of denaturation for 60 sec at 95°C and
293 annealing/extension for 60 sec at 58°C. The distribution of the quantitative RT-PCR mix containing SYBR
294 Green I Master (Roche), cDNAs and primers was performed using the EVO150© (Tecan) pipetting robot in
295 a 384-well plate. The expression of 43 genes, belonging to eight different physiological processes or
296 metabolic pathways (i.e. auxin, cytokinins, jasmonates, ethylene, salicylic acid, phenolic compounds,
297 reactive oxygen species (ROS), cell-division cycle), was quantified with specific primer pairs designed by
298 Quant-Prime [52] based on the *Populus trichocharpa* sequence (v3.0) from Phytozome
299 (https://phytozome.jgi.doe.gov/pz/portal.html; Table S2). Expression levels were normalized to the
300 levels of *PtUBIQUITIN10* (*PtUBQ10*), commonly used as a reference gene in plants [e.g. 53]. All RT-qPCR
301 experiments were done with three independent biological replicates, with two technical replicates each.
302 One of the biological replicates of the *M. persicae* – Koster interaction has been excluded from the
303 analyses because of technical issues during quantification. Relative gene expression was calculated
304 according to the $^{\Delta\Delta}$Ct method, with protoplasts incubated with protein extraction buffer as controls.
305 Primers used for gene expression analysis are listed in Table S2.

306

307 **2.3.5 Histochemical analysis of GUS activity**

308 Transgenic seedlings of *A. thaliana* (five-day-old and eight-day-old for *pIAA2*::GUS and *pARR16*::GUS,
309 respectively) were incubated with 2 mL of liquid MS containing 1 µg and 10 µg of aphid salivary proteins
310 (in TE/Tween buffer) of either *P. passerinii* or *M. persicae* for 3 h and 4 h for *pIAA2*::GUS and
311 *pARR16*::GUS, respectively. Positive controls were incubated with 20 µM of indole acetic acid (IAA)
312 (Sigma-Aldrich), and 20 µM of 6-benzylaminopurine (BAP) (Sigma-Aldrich). Negative controls were
313 incubated in liquid MS and corresponding volumes of TE/Tween buffer. Five seedlings were used for
314 each modality. Seedlings were then incubated in reaction buffer containing 0.1 M sodium phosphate
315 buffer (pH 7), 2 mM ferricyanide, 2 mM ferrocyanide, 0.1% (v/v) Triton X-100 and 1 mg ml^{-1} X-Gluc for
316 1 up to 24 h in dark at 37 °C. Afterwards, chlorophyll was removed by destaining in 70% ethanol and
317 seedlings were cleared as described by Malamy and Benfey [54]. GUS expression was monitored by
318 differential interference contrast microscopy.

319

320 **2.4 Data analysis**

321 All tests were carried out with the statistical software R 2.11.0 [55]. RT-qPCR results have been expressed
322 as fold-changes in gene expression compared to the reference gene *PtUBQ10*. Fold-changes have been
323 log_2 - transformed. Following this transformation, fold-changes varied between $-\infty$ and $+\infty$, with negative
324 values corresponding to gene underexpression, positive values to overexpression and zero, to no change
325 in gene expression. To visualize similarities and differences in fold-changes a heatmap was built, with
326 genes in columns and modalities in lines. The heatmap was built with a Z-score, i.e. log_2 – transformed
327 fold changes which have been normalized and centered per column. Hierarchical clustering, using
328 Pearson correlation as similarity metric, was performed to visualize the proximity among genes in
329 columns and among modalities in lines. The uncertainty of hierarchical clustering of modalities was

330 assessed with approximately unbiased p-values calculated with a multiscale bootstrap resampling, with
331 10,000 bootstrap replications, using the function pvclust() [56]. T-tests were performed with $^{\Delta}$Ct values
332 to detect significant changes in expression for each saliva treatment vs. controls. An analysis of variance,
333 followed with a Tukey test when significant, was also performed to compare the effect of treatment
334 modalities (i.e. aphid species and host genotype combinations) on log_2-fold changes of each gene.
335
336 **3 Results**
337
338 **3.1 Annotation, secreted proteins detection and identification**
339 From 36,312 and 3,233 transcripts, 1,243 and 221 transcripts were predicted to encode for secreted
340 salivary proteins in *P. passerinii* and *M. persicae*, respectively. About half of them (604) have been
341 annotated for *P. passerinii* and 190 for *M. persicae*. Using OrthoVenn, 121 and 58 protein clusters have
342 been identified for *P. passerinii* and *M. persicae*, respectively. About 17% of these clusters were common
343 between the two aphids (Table S3).
344 Blast2GO determined that *P. passerinii* salivary proteins were predominantly binding proteins and
345 enzymes (Fig. 1, table S4). The most common enzymes were peptidases (especially serine-type and
346 cysteine-type endopeptidases), kinases (especially phosphatidylinositol phosphate (PIP) kinases) and
347 hydrolases. Several enzymes involved in the degradation of carbohydrates (i.e. cellulase, trehalase, β-
348 glucuronidase, mannosidase and glucosylceramidase), and of phenolic compounds (i.e. peroxidase and
349 oxidoreductase) were also identified (Fig. 1, table S4). Among binding proteins, dimerization protein,
350 nucleic acids binding (especially DNA binding), nucleotide binding (especially ATP binding) and cation-
351 binding (mostly calcium ion-binding and zinc-binding proteins) were the most commonly found (Fig. 1,
352 table S4). Proteins related to hormone activity were also identified. Glucose dehydrogenases were also

353 detected with OrthoVenn (table S3). Among the 12 aphid salivary effectors considered, five were
354 identified in *P. passerinii*, with low E-values (< 7 e^{-71}): Mp10, ARMET, ACE 1, ACE2 and ACE3.
355
356 **3.2 Enzyme activities**
357 Staining with Coomassie blue confirmed the protein nature of the salivary sheath material (Fig. 2A) and
358 DOPA staining indicated a phenoloxidase activity in the sheaths (Fig. 2B). Black halos were also observed
359 around some sheaths (Fig. 2B). Likewise, peroxidase activity was found in salivary sheaths and halos
360 around sheaths (Fig. 2C). However, no pectinesterase, polygalacturonase and proteinase activity was
361 detected.
362
363 **3.3 Quantitative poplar gene expression**
364 An overview of poplar genes responses to aphid saliva is presented in figure 3. The hierarchical clustering
365 of modalities (left dendrogram) showed that all biological replicates of non-host interactions (i.e. *M.*
366 *persicae* – Koster and *M. persicae* – I-214) were grouped within a significant cluster, in which a majority
367 of poplar genes were upregulated following incubation with salivary proteins. Within this cluster,
368 replicates were not arranged according to poplar genotype. Biological replicates of the incompatible
369 interaction (i.e. *P. passerinii* – Koster) also clustered together, although the cluster was significant for
370 only two replicates. In this group, a majority of genes were weakly expressed and upregulated. For
371 biological replicates of the compatible interaction (i.e. *P. passerinii* – I-214), a majority were weakly
372 expressed and downregulated. Nonetheless, these replicates were not significantly clustered together.
373 The hierarchical clustering of genes (upper dendrogram) showed that there was no clustering of genes
374 according to physiological process or metabolic pathway.
375

376 For the auxin pathway, during non-host interactions (i.e. *M. persicae* – poplars) biosynthesis genes were
377 either not affected (*PtYUCCA*) or downregulated (*PtNIT1*) while *PtGH3*, which is involved in auxin inaction
378 via conjugation, was upregulated (Fig. 4). *PtAPB1* (signaling) and *PtPIN1* (auxin efflux carrier) were also
379 significantly upregulated, but only during the non-host interaction with I-214. No change was observed
380 in the expression of the auxin influx carrier *PtAUX1*. During incompatible interactions (i.e. *P. passerinii* –
381 Koster) these genes displayed an expression profile quite similar to that observed during non-host
382 interactions, except for *PtNIT1* whose expression was not affected by the salivary extracts of *P.*
383 *passerinii*. The expression of *PtGH3* was significantly downregulated during the compatible interaction,
384 and *PtGH3*, *PtAPB1* and *PtPIN1* were differentially expressed during the compatible interaction
385 compared to non-host interactions, and the incompatible interaction for *PtAPB1* only (Fig. 4).
386 For the cytokinin pathway, during non-host interactions with the poplar genotype I-214 *PtIPT*
387 (metabolism), *PtAHK4* (perception) and *PtARR2* (signaling) were upregulated while *PtLOG5* (metabolism)
388 was significantly downregulated (Fig. 4). A similar expression profile was observed during non-host
389 interactions with the poplar genotype Koster, but only *PtAHK4* and *PtLOG5* were significantly affected.
390 These genes were not significantly affected during the incompatible interaction. In contrast, *PtARR2* was
391 strongly repressed during the compatible interaction and *PtAHK4* and *PtARR2* were differentially
392 expressed during the compatible interaction compared to both non-host and incompatible interactions
393 (Fig. 4).
394 Regarding biotic stress signaling (i.e. jasmonates, salicylic acid, ethylene and ROS), non-host interactions
395 were characterized by a marked upregulation of a majority of genes, which was more frequently
396 significant for interactions with I-214 than for interactions with Koster (Fig. 5). Few genes in jasmonate
397 ethylene and ROS pathways were not affected by salivary extracts of *M. persicae* (i.e. *PtAOS*, *PtJAZ1*,
398 *PtEIN2*, *PtETO1*, *PtCAT* and *PtSOD*), and, in the salicylic acid pathway, *PtPR5* was significantly
399 downregulated. For interactions with *P. passerinii*, all genes were weakly downregulated during

400 compatible interactions. In contrast, during incompatible interactions most genes were either not
401 affected or evolved as during non-host interactions, with weak upregulations. Nonetheless, for these
402 modalities, no gene expression significantly differed from the controls (Fig. 5). In most situations, gene
403 expressions during compatible interactions were significantly lower than during non-host interactions
404 with I-214, and, in fewer situations, lower than during non-host interactions with Koster. Only *PtCOI1*
405 and *PtEIN3* genes were differentially expressed between compatible and incompatible interactions.
406 Conversely, since gene expressions during incompatible interactions were weakly upregulated, they
407 generally did not differ from those observed during non-host interactions with Koster, and differed from
408 non-host interactions with I-214 for only several genes (i.e. *PtCOI1*, *PtEDS1*, *PtNPR1*, *PtNDR1*, *PtEIN3*,
409 *PtADMS1*). Nonetheless, *PtPR5* and *PtSOD* were clearly differentially expressed between incompatible
410 and non-host interactions with Koster.
411 For genes involved in the phenolic compounds pathway (Fig. 5), non-host interactions led to an
412 upregulation of all the considered genes, especially for interactions with I-214. All genes were weakly,
413 but not significantly, downregulated or upregulated during compatible and incompatible interactions,
414 respectively. For all genes, expression was always significantly lower during the compatible interaction
415 compared to the non-host interaction with I-214. For *PtF5H*, expression was also significantly lower
416 during the compatible interaction compared to both non-host and incompatible interactions.
417 Finally, regarding genes involved in cell-division cycle, *PtCDK5*, *PtPCNA*, *PtCDK20 and PtE2F* were
418 significantly upregulated during non-host interactions, and while *PtCAK1* was significantly downregulated
419 (Fig. 6). *PtCYCD5* and *PtACO1* were also upregulated but only during non-host interactions with I-214.
420 Likewise, *PtCDK5* and *PtCDK20* were also significantly upregulated during the incompatible interaction,
421 as well as *PtCAK1*, conversely to non-host interactions. Expression of *PtMCM2* and *PtRBR* was not
422 affected by salivary extracts. *PtCDK20* was differentially expressed during the compatible interaction,
423 with a lower expression, compared to both incompatible and non-host interactions. Likewise, during the

424 incompatible interaction the expression of *PtCTR1* was much lower compared to non-host ones and
425 expression of *PtE3UL*, *PtE2F* and *PtACO1* were lower compared to expression during non-host
426 interactions with I-214. For *PtCAK1*, the expression was higher during the incompatible interaction than
427 during non-host ones.
428
429 **3.4 Histochemical analysis of GUS activity**
430 Salivary extracts of *P. passerinii* increased *pIAA2*::GUS signals (Fig. 7E, 7F, 7I, 7J), which were similar to
431 those caused by an exogenous application of auxin (Fig. 7A and 7B). Incubation with salivary proteins of
432 *M. persicae* resulted in faint colorations (Fig. 7G, 7H, 7K, 7L), similar to those of negative controls (Fig. 7C
433 and 7D).
434 Positive controls of *pARR16*::GUS were characterized by a strong staining in the middle part of root
435 central cylinder (Fig. 8A and 8B), which was weak in negative controls as well as with *M. persicae* salivary
436 proteins (Fig. 8G, 8H, 8K, and 8L). No coloration was visible in the roots of seedlings incubated with
437 salivary proteins of *P. passerinii* (Fig. 8E, 8F, 8I and 8J).
438
439 **4 Discussion**
440
441 Plant manipulation by parasites requires a finely tuned reprogramming of host metabolism, achieved
442 through secretion of effectors into the host plant [5, 7]. Using an *in vivo* approach with protoplasts, we
443 confirmed that salivary proteins impact plant gene transcription, strongly suggesting they mediate the
444 interactions between *P. passerinii* and its host-tree. This was further supported with a heterologous *in*
445 *planta* assay, with *A. thaliana*. Salivary extracts of *P. passerinii* weakly affected gene expression of the
446 two host-plant genotypes considered, but in a different way. During compatible interactions, in all the
447 metabolic pathways and physiological processes investigated, gene expressions were either unaffected

448 or weakly downregulated, except for the significant downregulation of two genes involved in
449 phytohormone pathways. Conversely, incompatible interactions generally led to weak upregulations,
450 significant for some genes related to cell-division cycle. As a result several genes involved in cytokinin
451 perception and signaling (*PtAHK4*, *PtARR2*), biotic stress signaling (*PtCOI1*, *PtEIN3*), defense (*PtF5H*) and
452 cell-division cycle (*PtCDK20*) were differentially expressed between compatible and incompatible
453 interactions. This supports the hypothesis that the saliva of *P. passerinii* includes effectors proteins
454 affecting plant signaling and defense mechanisms.
455
456 Several of the detected salivary proteins may interfere with plant signaling. PIP kinases were quite
457 abundant in the saliva of *P. passerinii*, but have not been previously reported from any aphid saliva.
458 These enzymes catalyze phosphorylation of phosphatidyl-inositol into phosphatidylinositol-4-5-
459 biphosphate (PIP_2). Hydrolysis of PIP_2 produces secondary messengers like diacylglycerol and inositol-1-
460 4-5-triphosphate (IP_3), which can in turn be hydrolyzed into phosphatidic acid (PA), considered an
461 important signaling molecule in plants, triggered in response to various biotic and abiotic stresses [57].
462 Likewise, PIP_2 and IP_3 can affect cellular oscillations of Ca^{2+} and are involved in multiple processes
463 including cell cycle and phytohormone regulation [58]. Other proteins, frequently detected in aphids,
464 may also interfere with secondary messengers like calcium-binding, ATP-binding, and GTP-binding
465 proteins or with hormone signaling like hormone-binding proteins [5, 12]. Likewise, it has been
466 hypothesized that trehalase may interfere with trehalose-based defense responses in *A. thaliana* [11],
467 and cellulases may also contribute to the degradation of oligogalacturonides involved in damage
468 signaling pathways [48]. Nucleic acid-binding proteins and protein-binding proteins could also participate
469 in the manipulation of host-plant metabolism [12]. Finally, oxidoreductases, especially peroxidases and
470 phenoloxidases could degrade phenolic compounds of the host plant [48; 59]. Pseudogall induction by *P.*
471 *passerinii* in susceptible host genotypes is characterized by transient accumulation of phenolic

472 compounds [24], and oxidoreductases could help aphids to cope with these secondary metabolites.
473 Glucose dehydrogenases may similarly help aphids to detoxify defensive compounds of the host-plant
474 [11, 59].
475 Many of the proteins detected in our study (e.g. calcium-binding, DNA-binding, ATP-binding, GTP-binding
476 proteins, glucose dehydrogenases, oxidoreductases, trehalases and phosphatases) have also been
477 previously identified in the saliva of different aphid species, which were sap-feeders [10, 11, 12, 47].
478 Therefore, although these proteins probably contribute to plant manipulation by aphids [47], they are
479 probably not specifically involved in pseudogall induction by *P. passerinii*. Interestingly, calcium-binding
480 proteins are supposedly key components of sap-feeding aphids' saliva, preventing the plugging of sieve
481 tubes [8]. Since *P. passerinii* does not feed on sap [23], it suggests that these proteins also play other
482 crucial roles during aphid-plant interactions. Several proteins detected in the saliva of *P. passerinii* such
483 as serine proteases, acid phosphatases, lipases and metalloproteases have been proposed as potential
484 effectors involved in formation and/or maintenance of fig wasps galls [60].
485 *In situ* biochemical assays confirmed the presence of peroxidases in both solid and soluble saliva of *P.*
486 *passerinii*. The phenoloxidase activity is also congruent with the numerous oxidoreductase sequences
487 identified in the salivary transcriptome. Likewise, the absence of pectin (methyl) esterase and
488 polygalacturonase activity during *in situ* bioassays is consistent with their absence in the salivary
489 transcriptome. However, while numerous proteases were identified among the salivary proteins of *P.*
490 *passerin*ii, no activity was observed during *in situ* bioassays. Gelatin was probably not the adequate
491 substrate to detect the protease activity of *P. passerinii*. Additional *in situ* assays could be conducted to
492 detect, in *P. passerinii* saliva, the activity of the proteases and possibly other enzymes like cellulases [43].
493 A proteomic analysis of salivary extracts should also confirm and complement the predictions of our
494 transcriptomic approach [13, 61].
495

496 To knock-down or divert stress signaling and/or ensure finely-tuned reprogramming of host metabolism
497 and anatomical transformation of host tissues, plant manipulation by herbivores or pathogens generally
498 requires reconfiguration of phytohormone pathways and signaling [62, 63]. Both RT-qPCR experiments
499 and histochemical assays confirmed that *P. passerinii* can actively manipulate phytohormone pathways
500 during compatible interactions. This is in line with the numerous proteins potentially interfering with
501 plant signaling and metabolism found in the aphid saliva. Salivary extracts of *P. passerinii* did not affect
502 either auxin biosynthesis or auxin transporter genes such as *PtPIN1* and *PtAUX1*, but significantly
503 downregulated *PtGH3*, which is involved in the homeostasis of auxin active forms [64]. This could lead to
504 intracellular accumulation of active auxin forms, and result in the targeted cell hypertrophy and
505 multiplication commonly observed during pseudogall differentiation by *P. passerinii* [24]. The activation
506 of the auxin-responsive promoter *IAA2* during *in planta* assays with transgenic seedlings of *A. thaliana*
507 further supports this hypothesis of an intracellular accumulation of auxin during gall initiation by *P.*
508 *passerinii*. Auxin accumulation, as a result of a reduction in both *GH3* activity and auxin transport, is also
509 probably involved in the initiation and development of root galls by cyst and root-knot nematodes [65].
510 Interestingly, the interaction between these plant-manipulating nematodes and their host-plants is also
511 rather associated with gene repression than with gene activation [15], as observed during compatible
512 interactions in our study, suggesting a potentially convergent manipulation strategy between these
513 organisms. As genes related to cytokinin biosynthesis (*PtIPT*) and activation (*PtLOG5*) were not affected
514 by salivary proteins of *P. passerinii*, the downregulation of cytokinin perception and signaling genes
515 (*PtAHK4* and *PtARR2* during the assays with protoplasts and *ARR16* during the assay with *A. thaliana*)
516 upon treatment during compatible interactions could correspond to an auxin accumulation-induced
517 regulation loop [66, 67]. Consequently, it could be hypothesized that *P. passerinii* manipulates auxin and
518 cytokinin plant responses to promote the host division cycle [62], leading to the formation of pseudogalls
519 (Fig. 9).

520

521 Apart from the Mp10 effector, the saliva of *P. passerinii* and *M. persicae* shared few similarities. The
522 transcriptomes of *P. passerinii* and *M. persicae* have been obtained with a different sequencing and
523 assembly methods [68]. This probably explains the difference in transcripts amounts gathered for both
524 aphids and several salivary proteins of *M. persicae* might be missing in its transcriptome, leading to an
525 apparently low similarity between secretomes. Likewise, the lack of biological replicates for both
526 transcriptomes might have also led to an underestimation of the similarity between secretomes.
527 However, previous comparisons among salivary proteins of aphid species also indicated that aphids with
528 different host species and / or feeding strategies exhibited very different salivary protein profiles [12,
529 69]. In addition to their difference in feeding strategy, the two aphid species are also phylogenetically
530 distant [27], which should further increase the dissimilarity of their secretomes. This is in agreement with
531 the markedly different gene expression profiles obtained for both aphid species.
532 Gene expression profiles of non-host interactions were significantly clustered together, independently of
533 poplar genotype. Conversely, gene expression profiles for interactions with salivary extracts of *P.*
534 *passerinii* differed according to host genotype, and incompatible interactions with Koster were grouped
535 together, apart from compatible interactions with I-214. In spite of the marked effect of aphid species,
536 gene expression profiles of poplar protoplasts during incompatible interactions with *P. passerinii* shared
537 many similarities with those observed during non-host interactions with *M. persicae*. Both types of
538 interactions were characterized by an overall upregulation of host genes, which was generally more
539 important during non-host interactions than during incompatible ones, for which only few significant
540 upregulations were observed. For most genes, expression during incompatible interactions did not differ
541 from those during non-host interactions with the same poplar genotype, Koster, but was occasionally
542 significantly lower than gene expression during non-host interactions with the other poplar genotype.
543 During both non-host and incompatible interactions, most genes involved in jasmonates, ethylene and

544 salicylic acid pathways tended to be upregulated, with significant upregulations for non-host interactions
545 only. All of these pathways can be activated following aphid feeding, together or separately, depending
546 on the aphid – plant interaction system considered [70, 71, 72]. Due to the salicylic acid - jasmonates
547 cross-talk, a differential gene expression between the two pathways could be expected [73], and this
548 could explain the downregulation of *PtPR5* during non-host interactions, but not the upregulation of
549 other genes related to the salicylic acid pathway. However, this may occur later during the interaction,
550 since in our experiments we only considered early gene responses [71]. As a consequence of activation
551 of plant defense signaling, genes related to secondary metabolism, i.e. *PtF3'5'H, PtANT* and *PtF5H* were
552 also upregulated during non-host interactions, and slightly upregulated during the incompatible
553 interactions. Conversely, the expression of these genes was either unaffected or slightly downregulated
554 during compatible interactions, which led to significantly lower expressions compared to the other
555 interactions. This is in agreement with previous histochemical analyses showing a light and transient
556 accumulation of phenolic compounds followed by their marked disappearance in manipulated tissues
557 during a compatible interaction, while their accumulation was strong and continuous during an
558 incompatible interaction [24].
559 Interestingly, two of the three genes that were differentially expressed during non-host and
560 incompatible interactions on the same poplar genotype (i.e. *PtPR5* and *PtSOD* – with a similar trend for
561 *PtCAT*) were related to biotic stress signaling, and were slightly upregulated during incompatible
562 interactions while they were significantly downregulated during non-host interactions. A similar
563 repression of *SOD* and *CAT* genes, leading to an increase in H_2O_2 content, together with an upregulation
564 of *PR1*, has been reported in potato leaves infested by *M. persicae* [71].
565 The putative intracellular accumulation of auxin during compatible interactions could also interfere with
566 salicylic acid signaling and defense responses [64], which is congruent with the overall absence of
567 response of genes related to the salicylic acid pathway. The downregulation of *PtAHK4* and *PtARR2* could

568 also interfere with stress signaling by preventing both accumulation of jasmonates and activation of
569 *PtPR1* [74], which is consistent with our observations during compatible interactions. As a result, the
570 effectors of *P. passerinii* saliva, in addition to modifying phytohormonal contents, probably down-
571 regulate the plant defenses to allow plant manipulation.
572 One of the first visible symptoms of pseudogall differentiation is cell multiplication in the cortical
573 parenchyma [24]. Nonetheless, exposure to the saliva of *P. passerinii* during compatible interactions did
574 not affect expression of genes involved in the cell-division cycle, or weakly downregulated them, while
575 most of these genes were upregulated during incompatible and non-host interactions. This is however
576 congruent with the fact that gall differentiation during the interactions between root-knot nematodes
577 and their host-plants is rather associated with gene repression than with gene activation [15]. The weak
578 downregulation might promote cell hypertrophy during compatible interactions. Additional experiments
579 considering genes coding for cell wall remodeling enzymes, activated early during giant cells
580 differentiation, or for cytoskeleton should provide further insight into the mechanisms associated with
581 the differentiation of hypertrophied cells [15].
582
583 In conclusion, our transcriptomic analysis of the saliva of *P. passerinii* and *M. persicae* showed that *P.*
584 *passerinii* probably secretes a highly peculiar saliva, filled with potential effectors that may interfere with
585 several plant secondary messengers and signaling pathways. Our *in vivo* approach with protoplasts and
586 *in planta* approach with a heterologous *A. thaliana*-system confirmed the ability of salivary extracts of
587 plant-manipulating insects to interfere with host response during compatible interactions. As expected
588 phytohormones pathways were affected, probably to impair biotic stress signaling but also to
589 reconfigure host metabolism and anatomy. Although the saliva of *P. passerinii* and *M. persicae* were very
590 different, incompatible and non-host interactions led to quite similar host responses, with a different
591 intensity however, and few differences in biotic stress signaling and cytokinin metabolism. Additional

592 modalities including different populations of *P. passerinii*, different poplar genotypes with intermediate
593 resistance levels, leading for instance to semi-compatible interactions [22], and additional host metabolic
594 pathways could be considered in future experiments. For instance, investigating how genes coding for
595 nucleotide-binding leucine-rich repeat (NB-LRR) proteins involved in the recognition of pathogens
596 effectors in poplar [75], and aphids in general [76], respond to salivary extracts of *P. passerinii* should
597 give further insights into the molecular processes underpinning failed and successful host manipulation
598 by a plant-manipulating organism.
599

600 **Funding**
601 This work was supported by the Région Centre-Val de Loire Project no. 2014 00094521 (InsectEffect)
602 coordinated by D. Giron.
603

604 **Acknowledgements**
605 We thank Léa Fléchon for her assistance with transcriptome analyses.
606

607 **References**
608

609 [1] L.M. Schoonhoven, J.J.A. Van Loon, M. Dicke, Insect–Plant Biology, Oxford University Press, 2005.
610 [2] F. Lieutier, K. Bermudez-Torres, J. Cook, M.O. Harris, L. Legal, A. Sallé, B. Schatz, D. Giron, From plant
611 exploitation to mutualism, in: N. Sauvion, D. Thiéry, P.A. Calatayud (Eds.), Insect-Plant Interactions in a
612 Crop Protection Perspective, Elsevier, 2017, pp. 55-109.
613 [3] G.N. Stone, K. Schönrogge, The adaptive significance of insect gall morphology. Trends Ecol. Evol., 18
614 (2003), 512-522.

615 [4] J.D. Shorthouse, D. Wool, A. Raman, Gall-inducing insects – nature's most sophisticated herbivores.
616 Basic Appl. Ecol., 6 (2005), 407-411.
617 [5] D. Giron, E. Huguet, G.N. Stone, M. Body, Insect-induced effects on plants and possible effectors
618 used by galling and leaf-mining insects to manipulate their host-plant. J. Ins. Physiol., 84 (2016), 70-89.
619 [6] J.F. Tooker, A.M. Helms, Phytohormone dynamics associated with gall insects, and their potential
620 role in the evolution of the gall-inducing habit. J. Chem. Ecol., 40 (2014), 742–753.
621 [7] S.A. Hogenhout, J.I. Bos, Effector proteins that modulate plant–insect interactions. Curr. Opin. Plant
622 Biol., 14 (2011), 422-428.
623 [8] T. Will, W.F. Tjallingii, A. Thönnessen, A.J. van Bel. Molecular sabotage of plant defense by aphid
624 saliva. Proc. Nat. Acad. Sci., 104 (2007), 10536-10541.
625 [9] A. Guiguet, G. Dubreuil, M.O. Harris, H. Appel, J.C. Schultz, M.H. Pereira, D. Giron, Shared weapons of
626 blood- and plant-feeding insects: surprising commonalities for manipulating hosts. J. Ins. Physiol., 84
627 (2016), 4–21.
628 [10] N. Harmel, E. Létocart, A. Cherqui, P. Giordanengo, G. Mazzucchelli, F. Guillonneau, E. De Pauw, E.
629 Haubruge, F. Francis, Identification of aphid salivary proteins: a proteomic investigation of *Myzus*
630 *persicae*. Ins. Mol. Biol., 17 (2008), 165–174.
631 [11] Nicholson S.J., Hartson S.D. & Puterka G.J. (2012). Proteomic analysis of secreted saliva from Russian
632 Wheat Aphid (*Diuraphis noxia* Kurd.) biotypes that differ in virulence to wheat. *Journal of Proteomics*, 75,
633 2252–2268.
634 [12] S. Vandermoten, N. Harmel, G. Mazzucchelli, E. De Pauw, E. Haubruge, F. Francis. Comparative
635 analyses of salivary proteins from three aphid species. Ins. Mol. Biol., 23 (2014), 67-77.
636 [13] H. Boulain, F. Legeai, E. Guy, S. Morlière, N.E. Douglas, J. Oh, M. Murugan, M. Smith, J. Jaquiéry, J.
637 Peccoud, F.F. White, J.C. Carolan, J.-C. Simon, A. Sugio,. Fast evolution and lineage-specific gene family

638 expansions of aphid salivary effectors driven by interactions with host-plants. Genome Biol. Evol., 10
639 (2018), 1554-1572.
640 [14] C. Zhao, L.N. Escalante, H. Chen, T.R. Benatti, J. Qu J., S. Chellapilla, …, S. Richards, A massive
641 expansion of effector genes underlies gall-formation in the wheat pest *Mayetiola destructor*. Curr. Biol.,
642 25 (2015), 613-620.
643 [15] B. Favery, M. Quentin, S. Jaubert-Possamai, P. Abad. Gall-forming root-knot nematodes hijack key
644 plant cellular functions to induce multinucleate and hypertrophied feeding cells. J. Ins. Physiol., 84
645 (2016), 60-69
646 [16] J.J. Stuart, M.S. Chen, R. Shukle, M.O. Harris, Gall midges (Hessian flies) as plant pathogens. Ann.
647 Rev. Phytopathol., 50 (2012), 339-357.
648 [17] C. Zhao, R. Shukle, L. Navarro Escalante, M.S. Chen, S. Richards, J.J. Stuart, Avirulence gene mapping
649 in the Hessian fly (*Mayetiola destructor*) reveals a protein phosphatase 2C effector gene family. J. Ins.
650 Physiol., 84 (2016), 22-31.
651 [18] N.S. Mutti, J. Louis, L.K. Pappan, K. Pappan, K. Begum, M.S. Chen, Y. Park, N. Dittmer, J. Marshall, J.C.
652 Reese, G.R. Reeck. A Protein from the salivary glands of the pea aphid, *Acyrthosiphon pisum*, is essential
653 in feeding on a host plant. Proc. Nat. Acad. Sci., 105 (2008), 9965-9969.
654 [19] H.S. Atamian, R. Chaudhary, V. Dal Cin, E. Bao, T. Girke, I. Kaloshian, *In planta* expression or delivery
655 of potato aphid *Macrosiphum euphorbiae* effectors Me10 and Me23 enhances aphid fecundity. Mol.
656 Plant-Microbe Int., 26 (2013), 67–74.
657 [20] De Vos M. & Jander G. (2009). *Myzus persicae* (green peach aphid) salivary components induce
658 defence responses in *Arabidopsis thaliana*. *Plant Cell & Environment*, 32, 1548–1560.
659 [21] R. Chaudhary, H.S. Atamian, Z. Shen, S.P. Briggs, I. Kaloshian, GroEL from the endosymbiont
660 *Buchnera aphidicola* betrays the aphid by triggering plant defense. Proc. Nat. Acad. Sci., 111 (2014),
661 8919-8924.

662 [22] A. Sallé, S. Pointeau, S. Bankhead-Dronnet, C. Bastien, F. Lieutier, Unraveling the tripartite
663 interactions among the woolly poplar aphid, its host tree, and their environment: a lead to improve the
664 management of a major tree plantation pest? Ann. For. Sci., 74 (2017), 79.
665 [23] S. Pointeau, A. Ameline, F. Laurans, A. Sallé, Y. Rahbé, S. Bankhead-Dronnet, F. Lieutier, Exceptional
666 plant penetration and feeding upon cortical parenchyma cells by the woolly poplar aphid. J. Ins. Physiol.,
667 58 (2012), 857–866.
668 [24] F. Dardeau, E. Deprost, F. Laurans, V. Lainé, F. Lieutier, A. Sallé, Resistant poplar genotypes inhibit
669 pseudogall formation by the wooly poplar aphid, *Phloeomyzus passerinii* Sign., Trees, 28 (2014), 1007-
670 1019.
671 [25] F. Dardeau, M. Body, A. Berthier, F. Miard, J. P. Christidès, M. Feinard-Duranceau, F. Brignolas, D.
672 Giron, F. Lieutier, A. Sallé, Effects of fertilisation on amino acid mobilisation by a plant-manipulating
673 insect. Ecol. Entomol., 40 (2015), 814-822.
674 [26] F. Dardeau, S. Pointeau, A. Ameline, F. Laurans, A. Cherqui, F. Lieutier, A. Sallé, Host manipulation by
675 a herbivore optimizes its feeding behaviour. Anim. Behav., 95 (2014), 49-56.
676 [27] Z. Ren, A.J. Harris, R.B. Dikow, E. Ma, Y. Zhong, J. Wen, Another look at the phylogenetic
677 relationships and intercontinental biogeography of eastern Asian–North American Rhus gall aphids
678 (Hemiptera: Aphididae: Eriosomatinae): Evidence from mitogenome sequences via genome skimming.
679 Mol. Phylogenet. Evol., 117 (2017), 102-110.
680 [28] A. Bishopp, S. El-Showk, D. Weijers, B. Scheres, J. Friml, E. Benková, A. Pekka Mähönen, Y. Helariutta,
681 A mutually inhibitory interaction between auxin and cytokinin specifies vascular pattern in roots. Curr.
682 Biol., 21 (2011), 917-926.
683 [29] T. Kiba, H. Yamada, T. Mizuno, Characterization of the ARR15 and ARR16 response regulators with
684 special reference to the cytokinin signaling pathway mediated by the AHK4 histidine kinase in roots of
685 *Arabidopsis thaliana*. Plant Cell Physiol., 43 (2002), 1059-1066.

686 [30] D. Zerbino, E. Birney, Velvet: algorithms for de novo short read assembly using de Bruijn graphs.
687 Gen. Res., (2008), gr-074492.
688 [31] M.H. Schulz, D.R. Zerbino, M. Vingron, E. Birney, Oases: robust *de novo* RNA-seq assembly across the
689 dynamic range of expression levels. Bioinformatics, 28 (2012), 1086-1092.
690 [32] Y. Yang, S.A. Smith, Optimizing *de novo* assembly of short-read RNA-seq data for phylogenomics.
691 BMC Genomics, 14 (2013), 328.
692 [33] O. Nishimura, Y. Hara, S. Kuraku S. gVolante for standardizing completeness assessment of genome
693 and transcriptome assemblies. Bioinformatics, 33 (2017), 3635-3637.
694 [34] D. Hyatt, G.L. Chen, P.F. LoCascio, M.L. Land, F.W. Larimer, L.J. Hauser, Prodigal: prokaryotic gene
695 recognition and translation initiation site identification. BMC Bioinformat., 11 (2010), 119.
696 [35] T.N. Petersen, S. Brunak, G. von Heijne, H. Nielsen, SignalP 4.0: discriminating signal peptides from
697 transmembrane regions, Nat. Methods, 8 (2011), 785.
698 [36] R. Ji, H. Yu, Q. Fu, H. Chen, W. Ye, S. Li, Y. Lou, Comparative transcriptome analysis of salivary glands
699 of two populations of rice brown planthopper, *Nilaparvata lugens*, that differ in virulence. PloS One, 8
700 (2013), e79612.
701 [37] J.D. Bendtsen, L.J. Jensen, N. Blom, G. von Heijne, S. Brunak, Feature-based prediction of non-
702 classical and leaderless protein secretion. Prot. Eng. Des. Sel., 17 (2004), 349-356.
703 [38] O. Emanuelsson, H. Nielsen, S. Brunak, G. von Heijne, Predicting subcellular localization of proteins
704 based on their N-terminal amino acid sequence. J. Mol. Biol., 300 (2000), 1005-1016.
705 [39] A. Pierleoni, P.L. Martelli, R. Casadio, PredGPI: a GPI-anchor predictor. BMC Bioinformat., 9 (2008),
706 392.
707 [40] A. Conesa, S. Götz, J.M. García-Gómez, J. Terol, M. Talón, M. Robles, Blast2GO: a universal tool for
708 annotation, visualization and analysis in functional genomics research. Bioinformat., 21 (2005), 3674–
709 3676.

710 [41] P. Jones, D. Binns, H.Y. Chang, M. Fraser, W. Li, C. McAnulla, H. McWilliam, J. Maslen, A. Mitchell, G.
711 Nuka, S. Pesseat, A.F. Quinn, A. Sangrador-Vegas, M. Scheremetjew, S.-Y. Yong, R. Lopez, S. Hunter,
712 InterProScan 5: genome-scale protein function classification. Bioinformat., 30 (2014), 1236-1240.
713 [42] Y. Wang, D. Coleman-Derr, G. Chen, Y.Q. Gu. OrthoVenn: a web server for genome wide comparison
714 and annotation of orthologous clusters across multiple species. Nucleic Acids Res., 43 (2015), W78-W84.
715 [43] S. Pundir, M.J. Martin, C. O'Donovan, Uniprot protein knowledgebase, in: C. Wu, C. Arighi, K. Ross
716 (Eds). Protein Bioinformatics. Methods in Molecular Biology, vol 1558. Humana Press, New York, 2017,
717 41-55.
718 [44] K. Guo, W. Wang, L. Luo, J. Chen, Y. Guo, F. Cui, Characterization of an aphid-specific, cysteine-rich
719 protein enriched in salivary glands. Biophys. Chem., 189 (2014), 25–32.
720 [45] M. Jaouannet, P.A. Rodriguez, P. Thorpe, C.J.G. Lenoir, R. MacLeod, C. Escudero-Martinez, J.I.B. Bos,
721 Plant immunity in plant–aphid interactions. Front. Plant Sci., 5 (2014), 663.
722 [46] Y. Pan, J. Zhu, L. Luo, L. Kang, F. Cui, High expression of a unique aphid protein in the salivary glands
723 of *Acyrthosiphon pisum*. Physiol. Mol. Plant Pathol., 92 (2015), 175–180.
724 [47] D.A. Elzinga, G. Jander, The role of protein effectors in plant–aphid interactions. Curr. Opin. Plant
725 Biol., 16 (2013), 451-456.
726 [48] A. Cherqui, W.F. Tjallingii, W.F. Salivary proteins of aphids, a pilot study on identification, separation
727 and immunolocalisation. J. Ins. Physiol., 46 (2000), 1177–1186.
728 [49] J.L. Yang, R. Yang, A.C. Cheng, R.Y. Jia, M.S. Wang, S.H. Zhang, Five-minute purification of PCR
729 products by new-freeze-squeeze method. J. Food Agric. Environ., 8 (2010), 32–33.
730 [50] M.E. Maffei, A. Mithöfer, W. Boland, Insects feeding on plants: rapid signals and responses
731 preceding the induction of phytochemical release. Phytochemistry, 68 (2007), 2946-2959.
732 [51] F.H. Wu, S.C. Shen, L.Y. Lee, S.H. Lee, M.T. Chan, C.S. Lin, Tape-*Arabidopsis* Sandwich-a simpler
733 *Arabidopsis* protoplast isolation method. Plant Meth., 5 (2009), 16.

734 [52] S. Arvidsson, M. Kwasniewski, D.M. Riaño-Pachón, B. Mueller-Roeber, QuantPrime--a flexible tool
735 for reliable high-throughput primer design for quantitative PCR. BMC Bioinformat., 9 (2008), 465.
736 [53] Z. Tong, Z. Gao, F. Wang, J. Zhou, Z. Zhang, Selection of reliable reference genes for gene expression
737 studies in peach using real-time PCR. BMC Mol. Biol., 10 (2009), 71.
738 [54] J.E. Malamy, P.N. Benfey, Organization and cell differentiation in lateral roots of *Arabidopsis*
739 *thaliana*. Development, 124 (1997), 33-44.
740 [55] R Core Team (2013). R: A language and environment for statistical computing. R Foundation for
741 Statistical Computing, Vienna, Austria. URL http://www.R-project.org/.
742 [56] R. Suzuki, H. Shimodaira, Pvclust: an R package for assessing the uncertainty in hierarchical
743 clustering. Bioinformatics, 22 (2006), 1540-1542.
744 [57] C. Testerink, T. Munnik, Phosphatidic acid: a multifunctional stress signaling lipid in plants. Trends
745 Plant Sci., 10 (2005), 368-375.
746 [58] H.W. Xue, X. Chen, Y. Mei, Function and regulation of phospholipid signalling in plants. Biochem. J.,
747 421 (2009), 145–156.
748 [59] J.C. Carolan, C.I.J. Fitzroy, P.D. Ashton, A.E. Douglas, T.L. Wilkinson, The secreted salivary proteome
749 of the pea aphid *Acyrthosiphon pisum* characterised by mass spectrometry. Proteomics, 9 (2009), 2457–
750 2467.
751 [60] E.O. Martinson, J.D. Hackett, C.A. Machado, A.E. Arnold, Metatranscriptome analysis of fig flowers
752 provides insights into potential mechanisms for mutualism stability and gall induction. PloS One, 10
753 (2015), e0130745.
754 [61] J.C. Carolan, D. Caragea, K.T. Reardon, N.S. Mutti, N. Dittmer, K. Pappan, F. Cui, M. Castaneto, J.
755 Poulain, C. Dossat, D. Tagu, J.C. Reese, G.R. Reeck, T.L. Wilkinson, O.R. Edwards, Predicted effector
756 molecules in the salivary secretome of the pea aphid (*Acyrthosiphon pisum*): a dual
757 transcriptomic/proteomic approach. J. Proteome Res., 10 (2011), 1505–1518.

758 [62] D. Giron, E. Frago, G. Glevarec, C.M. Pieterse, M. Dicke. Cytokinins as key regulators in plant–
759 microbe–insect interactions: connecting plant growth and defence. Funct. Ecol., 27 (2013), 599-609.
760 [63] J.F. Tooker, C.M. De Moraes Gall insects and indirect plant defenses: A case of active manipulation?
761 Plant Signal. Behav., 3 (2008), 503-504.
762 [64] J.E. Park, J.Y. Park, Y.S. Kim, P.E. Staswick, J. Jeon, J. Yun, S.-Y. Kim, J. Kim, Y.-H. Lee, C.M. Park. GH3-
763 mediated auxin homeostasis links growth regulation with stress adaptation response in *Arabidopsis*. J.
764 Biol. Chem., 282 (2007), 10036–10046.
765 [65] A. Karczmarek, H. Overmars, J. Helder, A. Goverse, Feeding cell development by cyst and root-knot
766 nematodes involves a similar early, local and transient activation of a specific auxin-inducible promoter
767 element. Mol. Plant Pathol., 5 (2004), 343-346.
768 [66] B. Jones, S.A. Gunnerås, S.V. Petersson, P. Tarkowski, N. Graham, S. May, K. Dolezal, G. Sandberg, K.
769 Ljung, Cytokinin regulation of auxin synthesis in *Arabidopsis* involves a homeostatic feedback loop
770 regulated via auxin and cytokinin signal transduction. The Plant Cell, 22 (2010), 2956-2969.
771 [67] G.E. Schaller, A. Bishopp, J.J. Kieber, The yin-yang of hormones: cytokinin and auxin interactions in
772 plant development. The Plant Cell, 27 (2015), 44-63.
773 [68] J.S. Ramsey, A.C.C. Wilson, M. de Vos, Q. Sun, C. Tamborindeguy, A. Winfield, G. Malloch, D.M.
774 Smith, B. Fenton, S.M. Gray, G. Jander, Genomic resources for *Myzus persicae*: EST sequencing, SNP
775 identification, and microarray design. BMC Genom., 8 (2007), 423–423.
776 [69] W.R. Cooper, J.W. Dillwith, G.J. Puterka, Comparisons of salivary proteins from five aphid
777 (Hemiptera: Aphididae) species. Environ. Entomol., 40 (2011), 151-156.
778 [70] I. Morkunas, V.C. Mai, B. Gabryś, Phytohormonal signaling in plant responses to aphid feeding. Acta
779 Physiol. Plant., 33 (2011), 2057–2073.

780 [71] P.I. Kerchev, B. Fenton, C.H. Foyer, R.D. Hancock, Infestation of potato (*Solanum tuberosum* L.) by
781 the peach-potato aphid (*Myzus persicae* Sulzer) alters cellular redox status and is influenced by
782 ascorbate. Plant Cell Environ, 35 (2012), 430-440.
783 [72] J. Louis, J. Shah. *Arabidopsis thaliana—Myzus persicae* interaction: shaping the understanding of
784 plant defense against phloem-feeding aphids. Front. Plant Sci., 4 (2013), 213.
785 [73] S.I. Zarate, L.A. Kempema, L.L. Walling. Silverleaf whitefly induces salicylic acid defenses and
786 suppresses effectual jasmonic acid defenses. Plant Physiol., 143 (2007), 866-875.
787 [74] J.A. O'Brien, E. Benková, Cytokinin cross-talking during biotic and abiotic stress responses. Front
788 Plant Sci., 4 (2013), 451.
789 [75] S. Hacquard, B. Petre, P. Frey, A. Hecker, N. Rouhier, S. Duplessis, The poplar-poplar rust interaction:
790 insights from genomics and transcriptomics. J. Pathogens, 2011 (2011), 1-11.
791 [76] F.L. Goggin, Plant–aphid interactions: molecular and ecological perspectives. Current opinion in
792 plant biology, 10 (2007), 399-408.

793 Figure 1: Gene Ontology treemap for the salivary transcriptome of *Phloeomyzus passerinii*. The box size
794 correlates to the number of sequences isolated. Numbers between brackets indicate the number of
795 sequences identified. Green boxes indicate binding proteins, purple boxes indicate enzymes, red boxes
796 indicate structural constituents, the blue box indicates transporters and the brown box molecular
797 transducers. The treemap was created with the treemap() function in R. A Detailed list of the proteins
798 can be found in the table S4.
799

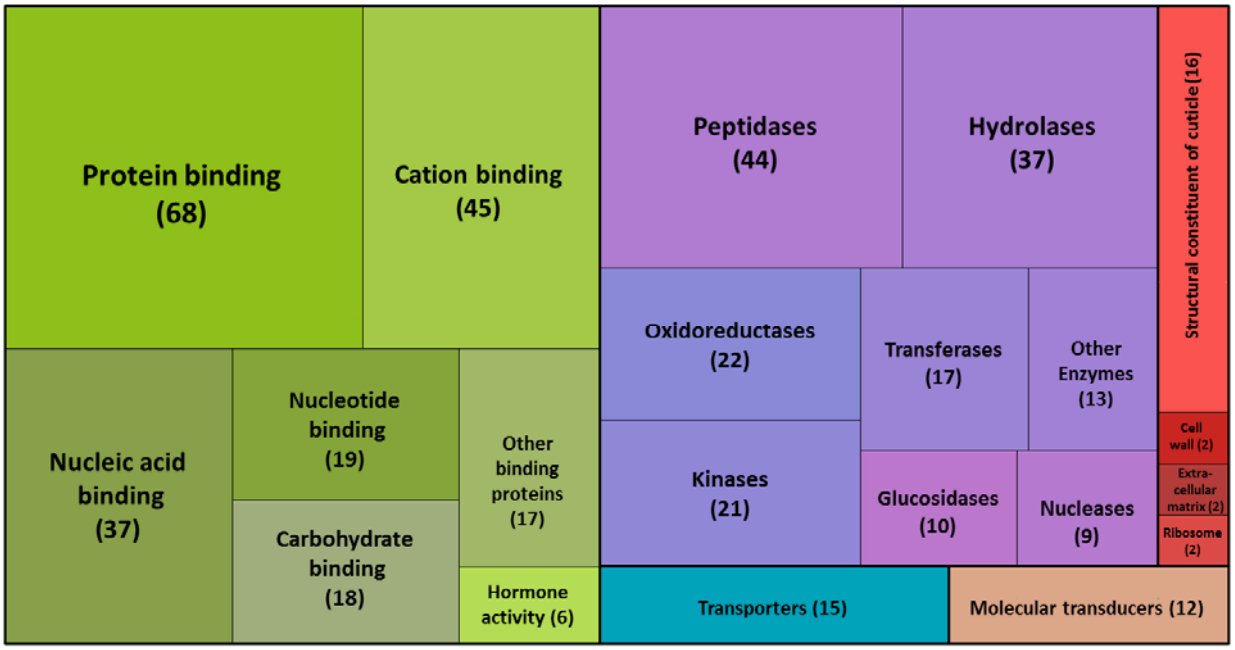

800
801

802 Figure 2: Representative salivary sheaths secreted in artificial diets by *Phloeomyzus passerinii*. Sheaths
803 stained and observed after 24 h probing in an agarose diet: (A) sheath stained with Coomassie blue; (B)
804 black stained sheaths in diet containing 0.1% DOPA, indicating a phenoloxidase activity, note the dark
805 halo surrounding the upper sheath; (C) reddish stained sheath in diet immersed with 0.1% DAB and 0.1%
806 H_2O_2, indicating a peroxidase activity. Black bars represent 10 µm.

807

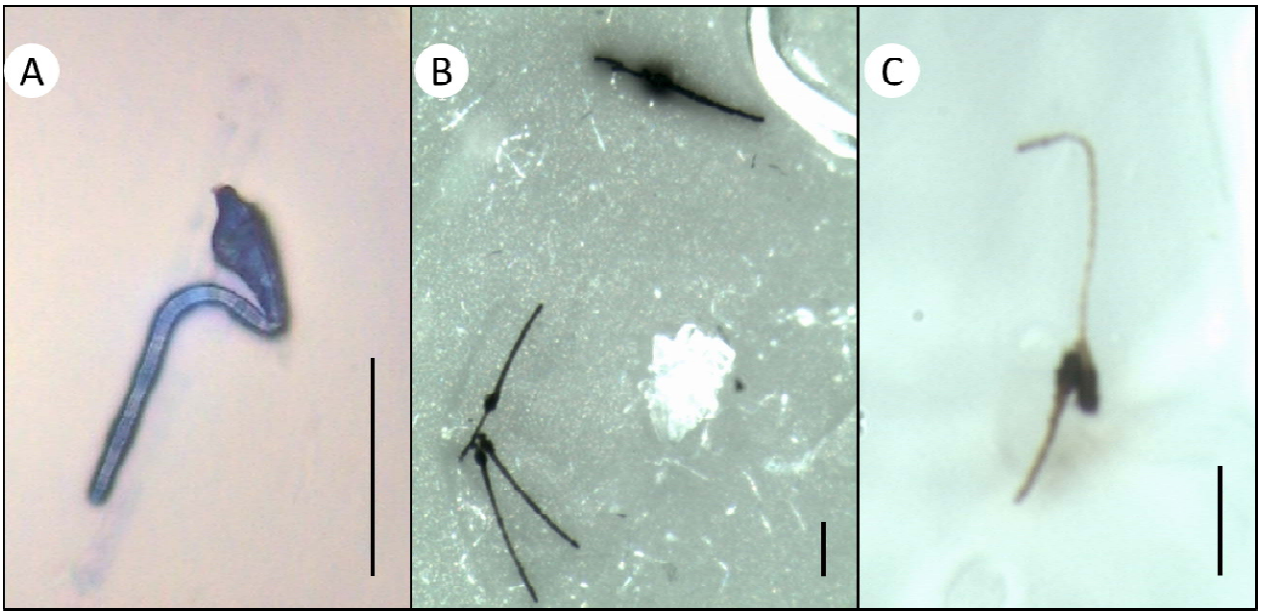

808

809

Figure 3: Heatmap of log_2-fold changes of 43 poplar genes belonging to eight different physiological processes or metabolic pathways (lower left box), after incubation of poplar protoplasts of two poplar genotypes (Koster and I-214) with salivary proteins of two aphids (*Myzus persicae* (*M. pers.*) and *Phloeomyzus passerinii* (*P. pass.*)). Non-host interactions are expected between both poplar genotypes and *M. persicae*, while incompatible interactions are expected between *P. passerinii* and Koster and compatible interactions between *P. passerinii* and I-214. Downregulation appears in blue and upregulation in red. Gene code is presented below the heatmap, modalities (i.e. aphid x poplar genotype combinations are presented on the right of the heatmap). Hierarchical clustering has been built with distances based on Pearson correlations. Approximately unbiased p-values (%) are indicated for the hierarchical clustering of modalities, red boxes indicate significant clusters at α = 0.05.

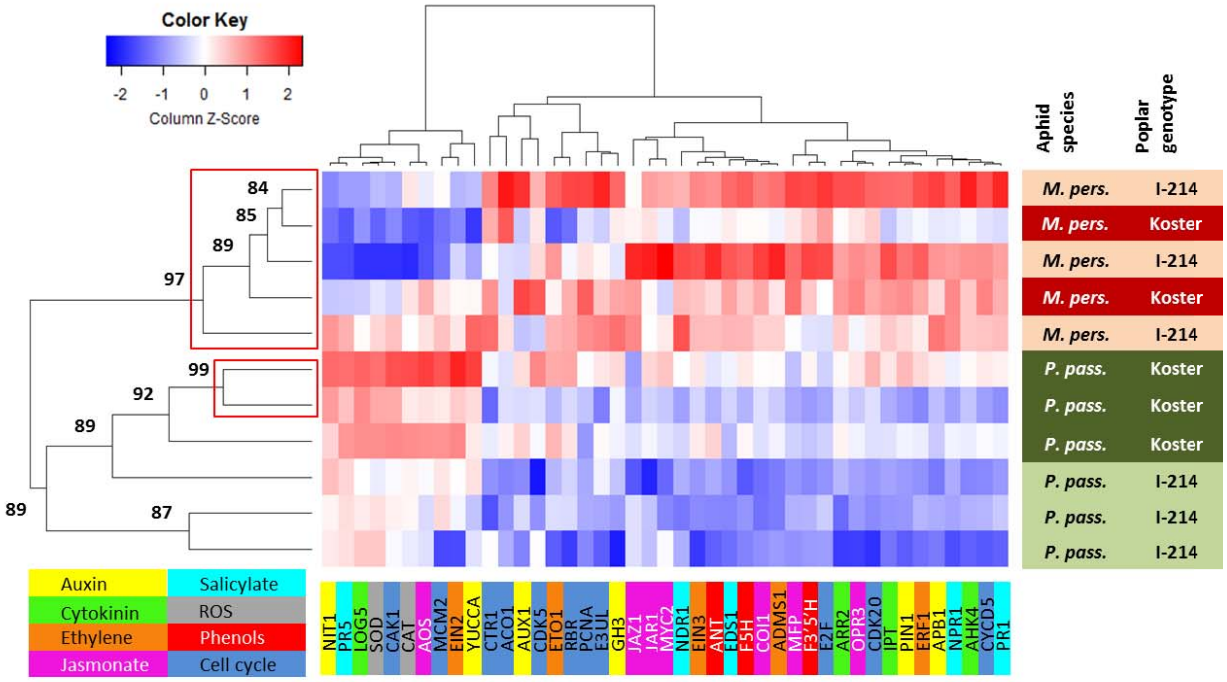

822 Figure 4: Mean (± SE) log_2-fold changes of genes involved in auxin (left) and cytokinin (right) pathways of
823 poplar protoplasts collected from two poplar genotypes (I-214 and Koster), after incubation with salivary
824 proteins of two aphids (*Myzus persicae* and *Phloeomyzus passerinii*), resulting in compatible,
825 incompatible and non-host interactions. Stars indicate modalities for which a significant upregulation or
826 downregulation of gene expression vs. controls was observed, using $^{\Delta}$Ct values (t-test). ***, ** and *
827 indicate a significant effect with P < 0.001, P < 0.01 and P < 0.05, respectively. Different letters indicate
828 significantly different groups (Tukey test) of log_2-fold changes among modalities, for each gene.
829

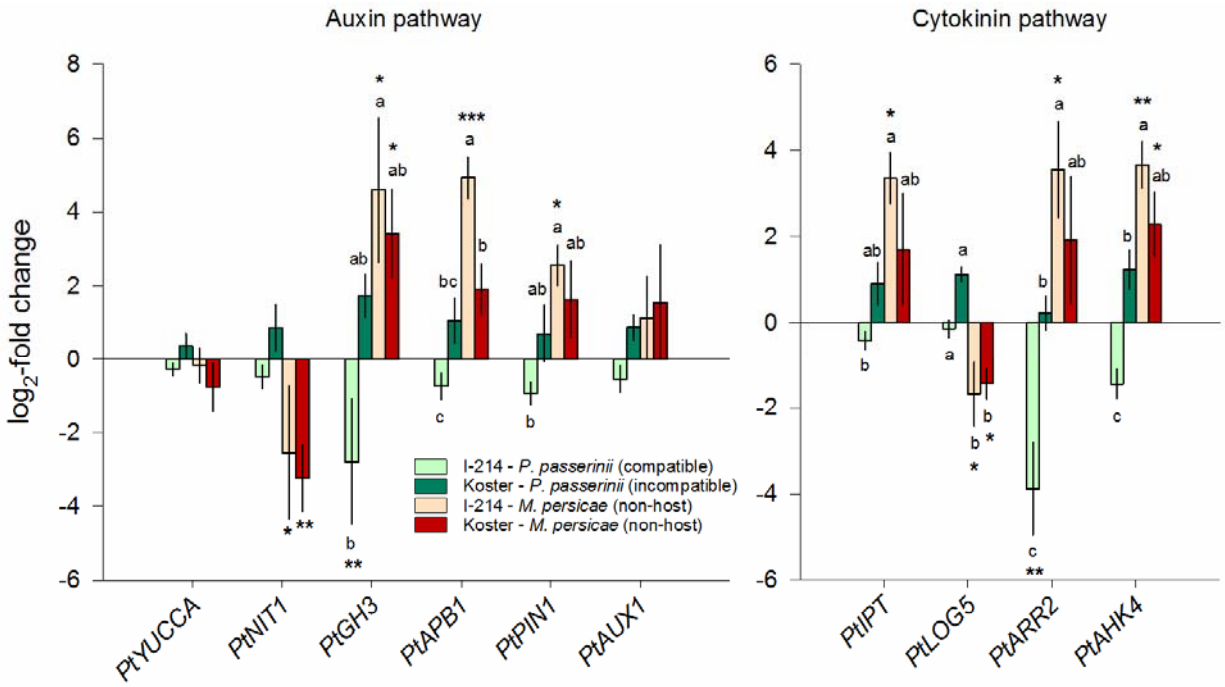

830
831

832 Figure 5: Mean (± SE) log_2-fold changes of genes involved in jasmonate, salicylic acid, ethylene pathways,
833 ROS responses and phenolic compounds of poplar protoplasts collected from two poplar genotypes (I-
834 214 and Koster), after incubation with salivary proteins of two aphids (*Myzus persicae* and *Phloeomyzus*
835 *passerinii*), resulting in compatible, incompatible and non-host interactions. Stars indicate modalities for
836 which a significant upregulation or downregulation of gene expression vs. controls was observed, using
837 $^{\Delta}$Ct values (t-test). ***, ** and * indicate a significant effect with P < 0.001, P < 0.01 and P < 0.05,
838 respectively. Different letters indicate significantly different groups (Tukey test) of log_2-fold changes
839 among modalities, for each gene.

840

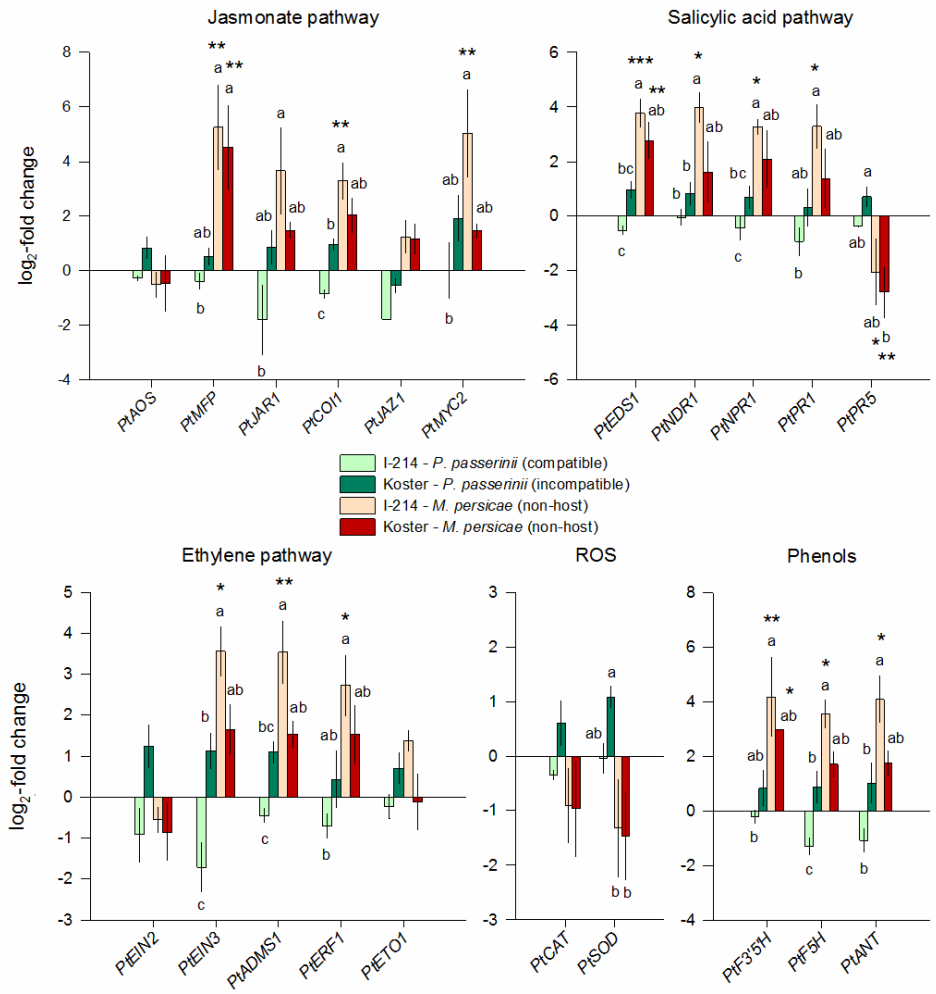

841

842 Figure 6: Mean (± SE) log_2-fold changes of genes involved in cell-division cycle of poplar protoplasts
843 collected from two poplar genotypes (I-214 and Koster), after incubation with salivary proteins of two
844 aphids (*Myzus persicae* and *Phloeomyzus passerinii*), resulting in compatible, incompatible and non-host
845 interactions. Stars indicate modalities for which a significant upregulation or downregulation of gene
846 expression vs. controls was observed, using $^{\Delta}$Ct values (t-test). ** and * indicate a significant effect with
847 $P < 0.01$ and $P < 0.05$, respectively. Different letters indicate significantly different groups (Tukey test) of
848 log_2-fold changes among modalities, for each gene.
849

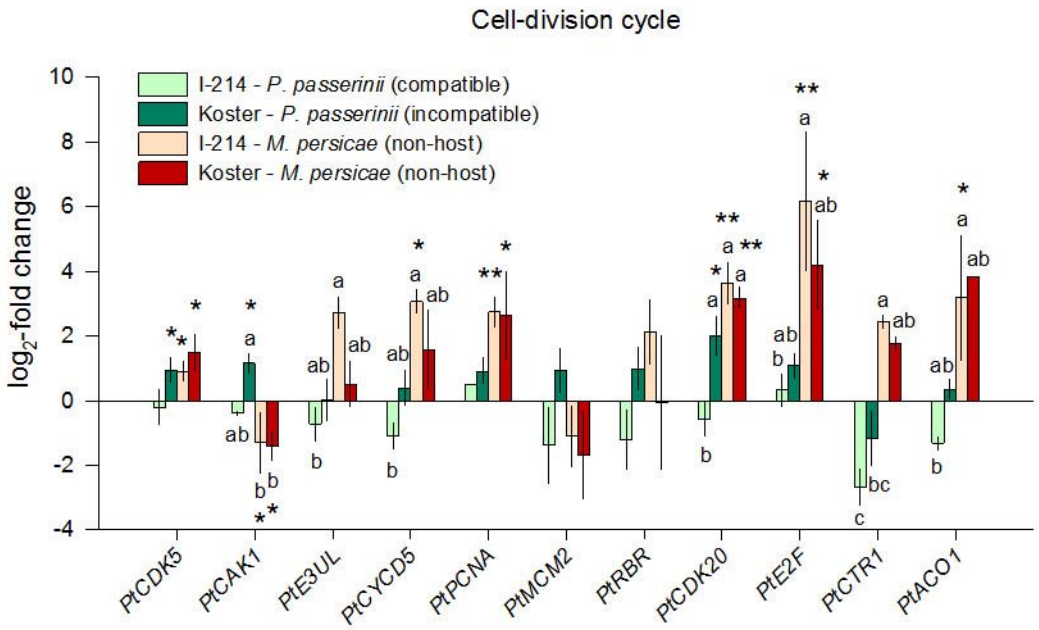

850

851 Figure 7: Representative GUS assays of transgenic seedlings of *Arabidopsis thaliana pIAA2*::GUS, showing

852 whole plants (A, C, E, G, I and K), and root tips (B, D, F, H, J and L), after 3 h of incubation in 20 µM of IAA

853 (A and B), TE/Tween buffer (C and D), and 1 and 10 µg of salivary proteins of *Phloeomyzus passerinii* (E, F,

854 I and J) or *Myzus persicae* (G, H, K and L). Black bars represent 1 mm for whole plants (A, C, E, G, I and K)

855 and 10 µm for root tips (B, D, F, H, J and L). Five seedlings were used for each modality.

856

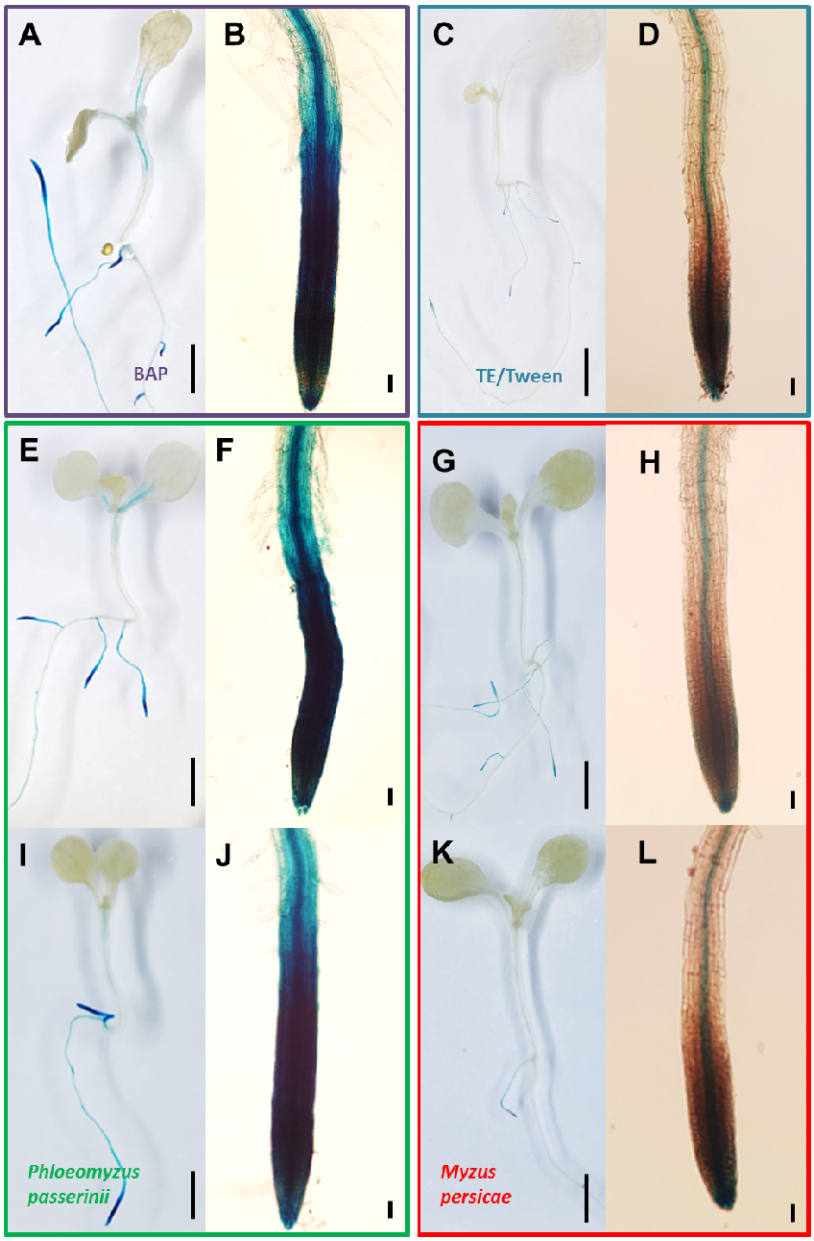

857

858

859 Figure 8: Representative GUS assays of transgenic seedlings of *Arabidopsis thaliana pARR16*::GUS,
860 showing whole plants (A, C, E, G, I and K), and root tips (B, D, F, H, J and L), after 4 h of incubation in 20
861 µM of BAP (A and B), TE/Tween buffer (C and D), and 1 and 10 µg of salivary proteins of *Phloeomyzus*
862 *passerinii* (E, F, I and J) or *Myzus persicae* (G, H, K and L). Black bars represent 1 mm for whole plants (A,
863 C, E, G, I and K) and 10 µm for root (B, D, F, H, J and L). Five seedlings were used for each modality.

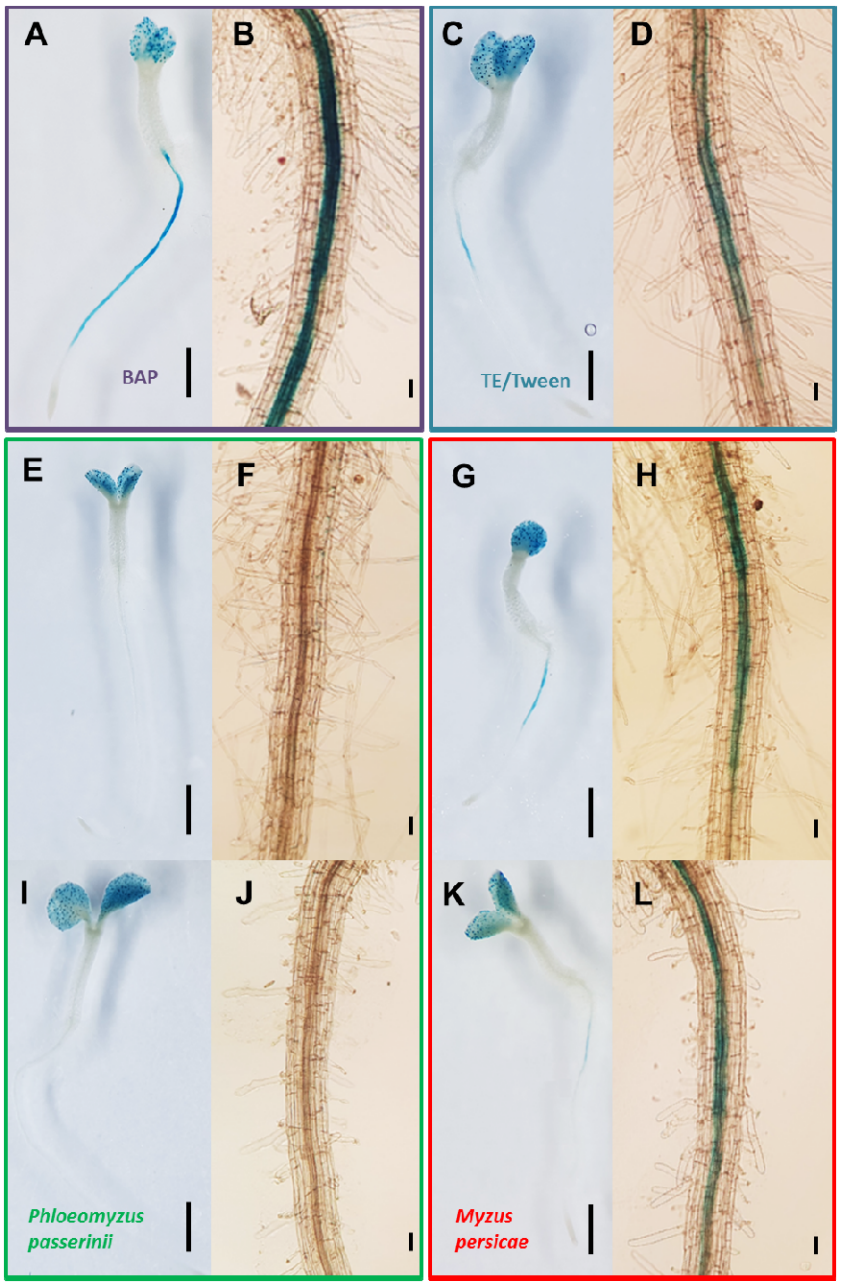

864

865 Figure 9: Graphical summary of effects of salivary extracts of *Phloeomyzus passerinii* on gene expression

866 in auxin and cytokinin pathways during a compatible interaction based on observations with *in vivo* RT-

867 qPCR assays with protoplasts (bold green) and heterologous *in planta* assay (bold orange).

868

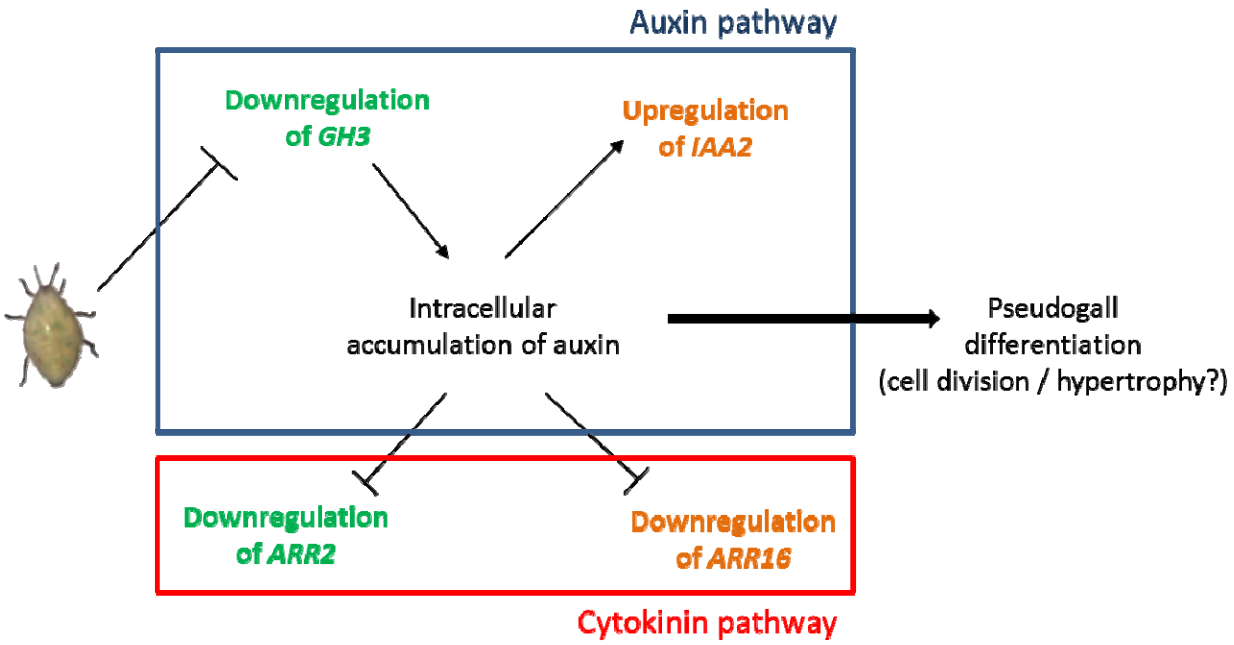

869

870 **Appendices**

871

872 Table S1. Illumina MiSeq sequencing and assembly statistics for *Phloeomyzus passerinii* salivary

873 transcriptome.

Number of raw read-pairs	15,453,942
Number of read-pairs after quality check*	11,578,269
Number of assembled transcripts	36,312
Average transcript length (bases)	858
N50 (bases)	1273
Transcriptome completeness (%)**	86.0 complete + 4.4 partial

874 * the reads were quality-clipped before performing the assembly with Trimmomatic v0.32. (Bolger *et al*. 2014).

875 ** assessed on 1066 core genes

Table S2. Genes considered for RT-qPCR, their sequence code in Phytozome and primers sequences.

Physiological process	Gene code	Sequence code	Protein	Primer fwd sequence	Primer rev sequence	Amplicon length	Tm	GC (%)	Optimal annealing temperature
Auxin	APB1	POPTR_0013s04160	Actin-binding protein ABP140	TCGTTTCCACCCATTCTTCTGTG	CACCACCCTCTTTAACATCTGAGG	128	61.3	48.9	60.3
Auxin	PIN1	POPTR_0007s14010	Peptidyl-prolyl cis-trans isomerase NIMA-interacting 1	GGGACTCAAGTTCGAGCATCACAC	TGGGTCTTTCCATGATGCCTTCC	75	63.6	53.2	60.1
Auxin	YUCCA	POPTR_0005s20840	Indole-3-pyruvate monoxygenase YUCCA11-related	CTGTACTGGATTGGCTGAAGGATG	CAGCACAGTAAAGCCCATTTCCC	65	61.7	47.9	58.2
Auxin	GH3	POPTR_0003s15970	Auxin-responsive GH3 family protein	GCCTTCGACTGCTGAAGAATTGG	TGGTCCAAGCCATCAACATACTTG	90	62.2	49.0	58.4
Auxin	AUX1	POPTR_0005s16020	Auxin influx carrier (AUX1 LAX family)	TGGCATGGTGGTTCAGTATGTG	TGAGAAGCACTTGTGCAACCTG	65	61.8	50.0	59.4
Auxin	NIT1	POPTR_0004s21160	Nitrilase-like protein 1	TGGTCTCCGCTCTCCAATTTGC	AGCAGCTCTAACCAATCTTTCAGC	80	62.6	50.2	61.4
Cytokinin	IPT	POPTR_0014s13540	TRNA delta 2 - isopentenylpyrophosphate transferase related	AGCAGAGCATGCCTGGGAAATG	AGAGGAGTTGTCCCACAATGGC	65	63.4	54.5	62.1
Cytokinin	AHK4	POPTR_0010s11350	Histidine kinase 4	GTGCTGACAGTGGTAAAGAAGCAC	GATACGACGTGTAGCCTCAAACCC	114	62.7	52.3	60.8
Cytokinin	LOG5	POPTR_0004s18850	Cytokinin riboside 5' - monophosphate PHOSPHORIBOHYDROLASE LOG5	TCTGCACCAAGTGCCAAAGAACTC	ATCATGCACAGGCACGTACTCCTC	60	64.6	52.1	59.0
Cytokinin	ARR2	POPTR_0014s12030	RESPONSE REGULATOR OF TWO-COMPONENT SYSTEM	GAAATGGATTTGCCTGTCGTCATC	AGCACCCTGAAGAACACCCTTC	78	62.0	50.2	58.1
Cell cycle	CDK5	POPTR_0006s05850	CDK5 REGULATORY SUBUNIT-ASSOCIATED PROTEIN 3	TTCATCATGGCCAAAGCAGGAAG	CATCAAACATGGACGAGAGTGTCC	79	62.5	51.0	60.8
Cell cycle	CAK1	POPTR_0018s09000	Pt-CAK1.2	AGCCTGCCTCCCTAATCATTCC	AGCTGGGTCATAGCAGACAAGC	70	62.6	54.5	60.8
Cell cycle	E3UL	POPTR_0003s20350	E3 UBIQUITIN LIGASE BIG BROTHER	ACTTGAATTAGGCGAGACAGTTGG	TGGCAAATGACACACCTCTCAC	138	61.4	47.9	60.8
Cell cycle	CYCD5	POPTR_0014s01700	CYCLIN-D5-1	GGCTAATCGAGAGCCTCATCAAGG	CAAGCGGGCAGTTCTAAACGAG	79	62.8	54.4	59.5
Cell cycle	PCNA	POPTR_0001s25490	PROLIFERATING CELL NUCLEAR ANTIGEN	ACACCACAGTTGATAAGCCGGAAG	GAAGGAGTTCATGTACCTCAGTGC	62	62.9	50.0	59.2
Cell cycle	MCM2	POPTR_0006s02620	MINICHROMOSOME MAINTENANCE (MCM2/3/5) FAMILY PROTEIN	AGGAATAAACCCAATTCCCAACGC	AGTGTGCTTCCCTCTACCACTTC	77	62.8	49.0	60.0
Cell cycle	RBR	POPTR_0001s06870	RETINOBLASTOMA-ASSOCIATED PROTEIN RB –RELATED	TGCTGGTGGATGTTGGTTCTGC	AGGTGATGCAGGACATTGACCATC	95	63.7	52.3	60.3
Cell cycle	CDK20	POPTR_0091s00250	CYCLIN-DEPENDENT KINASE 20	TGGAGATAAGCTGGTGCTCACTG	CCTATACGCAATGGTAGTGACCTG	97	61.9	51.1	61.6
Cell cycle	E2F	POPTR_0015s08160	E2F TRANSCRIPTION FACTOR-LIKE E2FE	ATCTCACTCGATGAATCTGCCAAG	CTTGTATCAGCAGTGTGGGTCTTC	146	61.4	47.9	60.2

884 Table S2 cont.

Physiological process	Gene code	Sequence code	Protein	Primer fwd sequence	Primer rev sequence	Amplicon length	Tm	GC (%)	Optimal annealing temperature
Ethylene	CTR1	POPTR_0016s11050	serine/threonine-protein kinase CTR1	TGAGTCTTGCTGGGCCAATGAAC	TCATGCCTGCAAGACCAGGTTG	113	63.8	53.4	63.0
Ethylene	ACO1	POPTR_0004s00460	Aminocyclopropanecarboxylate oxidase	TGGAGGTGATCAATGATGCCTGTG	ATCCCATGGTTCACCAACTCAAAG	60	62.4	48.9	58.7
Ethylene	EIN3	POPTR_0001s05360	ETHYLENE-INSENSITIVE3-like 3 protein	AACTGCAGCGCAACCATTTCTG	ACAACTGTTAAGGCAGCACCTC	74	62.3	50.0	58.9
Ethylene	ADMS1	POPTR_0014s11000	S-adenosylmethionine synthetase 1	TCGTAGGTGCATTGTGCAAGTC	TGCCATAGGTGTCCACAAAGACAG	79	62.5	50.0	60.8
Ethylene	ERF1	POPTR_0001s36610	Ethylene responsive element binding factor 3	CTTCTTCTTTGTGCCGCAAGCC	ATCACCAGAGCCCAAGTCAACC	80	63.2	54.5	61.3
Ethylene	EIN2	POPTR_0016s09210	ethylene-insensitive protein 2	TAAGCGAGGAGAGTGTGTTTGCC	ATTTGGTGGTCCCTGATGTTGCAG	109	63.6	52.2	61.7
Ethylene	ETO1	POPTR_0016s13180	ETO1-LIKE PROTEIN 2-RELATED	CTCTATAAGAGAGCACGGGAACGG	TTTCCCTGAGGAACACTGGCTCTC	67	63.6	54.2	59.6
Jasmonic acid	AOS	POPTR_0004s15600	allene oxide synthase	TGAACCTCCGGTTCCATTCCAG	ATAGGCCGCGTGATGACTTTCG	73	63.1	54.5	61.0
Jasmonic acid	JAZ1	POPTR_0001s16640	jasmonate ZIM domain-containing protein	TGAAGCGCCTAACGGTTCAGATG	GGAGAAGAACCGATGAAGTGATGC	64	62.9	51.1	59.8
Jasmonic acid	MFP	POPTR_0010s01570	MULTIFUNCTIONAL PROTEIN	GGAAGGAAGCAGGACTAAGGGAAG	GTCCTTCAAGCTGTACAACACGTC	124	62.6	52.1	61.9
Jasmonic acid	JAR1	POPTR_0014s09120	jasmonic acid-amino synthetase	GAGTGTTGCAATTGCCTGGATCG	ATGGCCTTCACCTTCCGTGAAC	71	63.3	53.4	60.6
Jasmonic acid	MYC2	POPTR_0002s17750	transcription factor MYC2	CGTGAACAGAAGAACGCTCGTG	AAGACAGGCCTGGTTTATTAGCG	70	62.0	51.2	58.1
Jasmonic acid	COI1	POPTR_0008s06460	CORONATINE INSENSITIVE 1	AGCACTTCCGCTCTAGGTACAC	AGGTTAAGCTAACTGCCACAGACG	61	62.7	52.3	58.8
Jasmonic acid	OPR3	POPTR_0018s07120	12-oxophytodienoate reductase	ACAAGATGTAGGGCGTTGAATGGG	TTCCAGGCACATGAGGAAACCC	142	63.4	52.3	65.7
Phenolics	F3'5'H	POPTR_0007s06300	Flavonoid 3',5'-hydroxylase / F3'5'H	GCTGCGAAGCATATCTCTTACGTG	ACGCATGCCCTCATGAATCAC	139	62.4	52.3	61.6
Phenolics	ANT	POPTR_0001s40590	Anthocyanin 5-O-glucoside 6'''-O-malonyltransferase	AAGTCGTTTAGACCCTCCTCTTCC	ATGTGACGAGCCACAACAGTATC	63	61.6	48.9	57.9
Phenolics	F5H	POPTR_0007s13720	ferulate-5-hydroxylase	TGATGTTTGGTGGGACAGAGACG	TCTTCATTAGCTCCGCCATGACC	66	63.0	52.2	61.6
ROS	SOD	POPTR_0005s09190	SUPEROXIDE DISMUTASE	GATTTCAACAATGCTGCCCAGGTC	TGCCAAGTTCTGGCATGTCTCC	66	62.7	51.1	57.8
ROS	CAT	POPTR_0005s27300	CATALASE 3	TTCTGCTGTCTGCAGTGGAAGG	CGAACGAAACGTTCTTGCCTGTC	113	62.9	54.5	62.9
Salicylic acid	PR1	POPTR_0001s29530	Pathogenesis-related protein	CTACGTCAATGCCCACAATAATGC	CTGCCACATTAGTGTCCCAGAC	74	61.2	50.2	59.6
Salicylic acid	EDS1	POPTR_0015s08100	ENHANCED DISEASE SUSCEPTIBILITY 1	GAATGACCTAGGCCTGAGTGAAAG	TTCTCTAACGCTTCAGCAGCAC	63	61.4	50.0	59.7
Salicylic acid	NPR1	POPTR_0014s11120	NPR1 interacting (NPR1_interact)	CCCTGCATACAACAACCAACAAC	TCGCGAATGCCCTTGATGAG	137	61.2	51.4	60.2
Salicylic acid	PR5	POPTR_0005s26240	receptor serine/threonine kinase PR5K	ACAGCTACACACCACTCGTCAAC	AGATGGCGATGCTCCATTCTGG	71	63.4	53.4	60.6
Salicylic acid	NDR1	POPTR_0012s12790	NDR1/HIN1-LIKE	GCAACAACTGCAGGCTGGAATC	AGCTTGATTCTCACAGGCTGGTC	62	62.9	54.5	60.2

885

886

887 Table S3 Number of orthologous proteins between the salivary transcriptomes of *Phloeomyzus passerinii*

888 and *Myzus persicae.*

889

Proteins	***P. passerinii***	***M. persicae***
phosphatidylinositol-4-phosphate 5-kinase	16	0
Glucose dehydrogenase [FAD, quinone]	8	0
Gut esterase 1	8	0
Serine protease	7	0
Furin-like protease	6	0
Transcription factor SPT20 homolog	6	0
Phospholipase A1	5	0
Probable serine/threonine-protein kinase nek3	5	0
cuticle precursor	4	0
Protein Toll	4	0
tyrosine kinase receptor	4	0
Acetylcholine receptor	3	0
Activating signal cointegrator 1 complex subunit 2 homolog	3	0
Down syndrome cell adhesion molecule-like protein Dscam2	3	0
Fibroin heavy chain	3	0
leucine-rich repeat containing G-coupled receptor	3	0
Peritrophin-1	3	0
zinc metallo ase nas-13-like	2	0
60S ribosomal protein L27a	2	0
AF4 FMR2 family member 4-like	2	0
Basement membrane proteoglycan	2	0
cell wall DAN4	2	0
C-type lectin-like precursor	2	0
Cuticle protein	2	0
Cuticle protein 19	2	0
Diuretic hormone	2	0
DNA-directed RNA polymerase II subunit RPB1-like	2	0
Dolichyldiphosphatase 1	2	0
endocuticle structural glyco bd-8-like	2	0
Endocuticle structural glycoprotein SgAbd-2	2	0
Endoglucanase	2	0
Extensin	2	0
glia-derived nexin	2	0
Heterogeneous nuclear ribonucleoprotein A1	2	0
Hypertrehalosaemic prohormone	2	0
hypothetical protein WALSEDRAFT_31439	2	0
Low-density lipoprotein receptor-related protein	2	0
Maltase A2	2	0
mesencephalic astrocyte-derived neurotrophic factor homolog	2	0
multiple epidermal growth factor-like domains 10	2	0
Neurogenic locus Notch protein	2	0
Neuropeptide CCHamide-1	2	0
nose resistant to fluoxetine 6- partial; nose resistant to fluoxetine 6-like	2	0
odorant binding 10	2	0
odorant binding 9	2	0
PREDICTED: meteorin-like protein	2	0
PREDICTED: spondin-1-like	2	0
Probable G-protein coupled receptor Mth-like 1	2	0
probable serine threonine- kinase nek3	2	0

890

891 Table S3 cont.

Protein yellow	2	0
proto-oncogene tyrosine- kinase ROS	2	0
Putative UDP-glucuronosyltransferase ugt-47	2	0
synaptic vesicular amine transporter isoform X1	2	0
Thioredoxin domain-containing protein	2	0
transmembrane emp24 domain-containing bai-like isoform X2	2	0
Transmembrane emp24 domain-containing protein A	2	0
uncharacterized family 31 glucosidase KIAA1161-like	2	0
Angiotensin-converting enzyme	1	0
Beta-amyloid-like protein	1	0
canopy homolog 4-like precursor	1	0
Cathepsin L	1	0
flocculation FLO11-like	1	0
prostatic spermine-binding -like	1	0
Protein 60A	1	0
Putative acid phosphatase 5	1	0
Slit homolog 1 protein	1	0
sulfhydryl oxidase 2-like	1	0
Translocon-associated protein subunit alpha	1	0
Cathepsin B-like cysteine proteinase 4	5	1
Chorion peroxidase	5	2
esterase E4-like isoform X1	5	1
carbonic anhydrase 7-like	3	1
Collagen alpha-1(IV) chain	2	1
cathepsin D	2	1
Vitellogenin-1	2	1
Ejaculatory bulb-specific protein 3	1	3
Protein takeout	1	1
15 kDa seleno -like precursor	1	1
Probable sodium/potassium/calcium exchanger CG1090	1	1
Phosphatidylethanolamine-binding protein homolog F40A3.3	1	1
Neuroglian	1	1
Cuticle protein 18.6, isoform B	1	1
WD repeat-containing 18	1	1
transmembrane emp24 domain-containing eca	1	1
Translocon-associated protein subunit beta	1	1
PREDICTED: uncharacterized protein LOC100160421	1	1

892 Table S4

893 Gene ontology annotations of genes from salivary glands of *Phloeomyzus passerinii*. All genes belonged
894 to the Molecular Function category.

Gene Ontology (GO)	Number of sequences
protein binding	55
nucleic acid binding	19
structural constituent of cuticle	16
phosphatidylinositol phosphate kinase activity	15
serine-type endopeptidase activity	15
zinc ion binding	13
chitin binding	13
DNA binding	13
metal ion binding	12
calcium ion binding	12
odorant binding	9
ATP binding	9
hydrolase activity	7
protein dimerization activity	7
hormone activity	6
oxidoreductase activity	6
cysteine-type endopeptidase activity	6
peroxidase activity	5
metalloendopeptidase activity	5
nucleotide binding	5
heme binding	5
carboxylic ester hydrolase activity	4
DNA-binding transcription factor activity	4
peptide-methionine (S)-S-oxide reductase activity	4
protein-hormone receptor activity	3
triglyceride lipase activity	3
nuclease activity	3
RNA binding	3
N-acetyltransferase activity	3
catalytic activity	3
transporter activity	3
acetylcholine-gated cation-selective channel activity	3
transferase activity, transferring hexosyl groups	3
hydrolase activity, hydrolyzing O-glycosyl compounds	3
peptidase activity	3
chitinase activity	3
metallopeptidase activity	3
aspartic-type endopeptidase activity	2
3'-5' exonuclease activity	2
serine-type endopeptidase inhibitor activity	2
hydrolase activity, acting on glycosyl bonds	2
oxidoreductase activity, acting on CH-OH group of donors	2
cellulase activity	2
leucine-tRNA ligase activity	2
structural constituent of cell wall	2
acid phosphatase activity	2
G-protein coupled receptor activity	2
heparin binding	2
scavenger receptor activity	2
sulfuric ester hydrolase activity	2
cation binding	2
protein tyrosine kinase activity	2
growth factor activity	2
transferase activity	2

895 Table S4 cont.

896

extracellular matrix structural constituent	2
transition metal ion binding	2
carbohydrate binding	2
obsolete signal transducer activity	2
cholinesterase activity	2
RNA-DNA hybrid ribonuclease activity	2
iron ion binding	2
aminoacyl-tRNA editing activity	2
serine-type peptidase activity	2
GTP binding	2
transferase activity, transferring glycosyl groups	2
flavin adenine dinucleotide binding	2
structural constituent of ribosome	2
G-protein beta/gamma-subunit complex binding	1
cysteine-type peptidase activity	1
mRNA binding	1
DNA-directed 5'-3' RNA polymerase activity	1
transmembrane receptor protein serine/threonine kinase activity	1
lysozyme activity	1
unfolded protein binding	1
omega peptidase activity	1
iron-sulfur cluster binding	1
alpha,alpha-trehalase activity	1
protein kinase binding	1
sequence-specific DNA binding	1
voltage-gated potassium channel activity	1
endopeptidase inhibitor activity	1
transmembrane transporter activity	1
protein kinase activity	1
copper ion binding	1
DNA-directed DNA polymerase activity	1
endonuclease activity	1
carboxypeptidase activity	1
O-acyltransferase activity	1
hedgehog receptor activity	1
isomerase activity	1
proton transmembrane transporter activity	1
GTPase activator activity	1
cis-stilbene-oxide hydrolase activity	1
carbonate dehydratase activity	1
metallocarboxypeptidase activity	1
cation transmembrane transporter activity	1
phosphatase activity	1
extracellular ligand-gated ion channel activity	1
cysteine dioxygenase activity	1
ion channel inhibitor activity	1
transmembrane receptor protein tyrosine kinase activity	1
protein heterodimerization activity	1
polysaccharide binding	1
G-protein coupled receptor binding	1
1-alkyl-2-acetylglycerophosphocholine esterase activity	1
sulfotransferase activity	1
ATPase activity, coupled to transmembrane movement of substances	1

897

898

899 Table S4 cont.

	900
ubiquitin protein ligase binding	1
phospholipase A2 activity	1
poly(A)-specific ribonuclease activity	1
obsolete signal transducer, downstream of receptor, with serine/threonine kinase activity	1
glucosylceramidase activity	1
hydrolase activity, acting on carbon-nitrogen (but not peptide) bonds	1
ionotropic glutamate receptor activity	1
signaling receptor binding	1
GPI-anchor transamidase activity	1
extracellularly glutamate-gated ion channel activity	1
dolichyl-diphosphooligosaccharide-protein glycotransferase activity	1
thiol oxidase activity	1
phosphatidylinositol N-acetylglucosaminyltransferase activity	1
ion channel activity	1
oxidoreductase activity, acting on the aldehyde or oxo group of donors, NAD or NADP as acceptor	1
peptidyl-dipeptidase activity	1
FMN binding	1
electron transfer activity	1
lipid transporter activity	1
transferase activity, transferring acyl groups other than amino-acyl groups	1
beta-glucuronidase activity	1
alpha-mannosidase activity	1
GTPase activity	1
hydrolase activity, acting on carbon-nitrogen (but not peptide) bonds, in linear amides	1
protein serine/threonine kinase activity	1
succinate dehydrogenase activity	1
mannosyl-oligosaccharide 1,2-alpha-mannosidase activity	1

901 Figure S1: Pipeline for the annotation process. Data are in orange, analyses in blue, results in green.

902

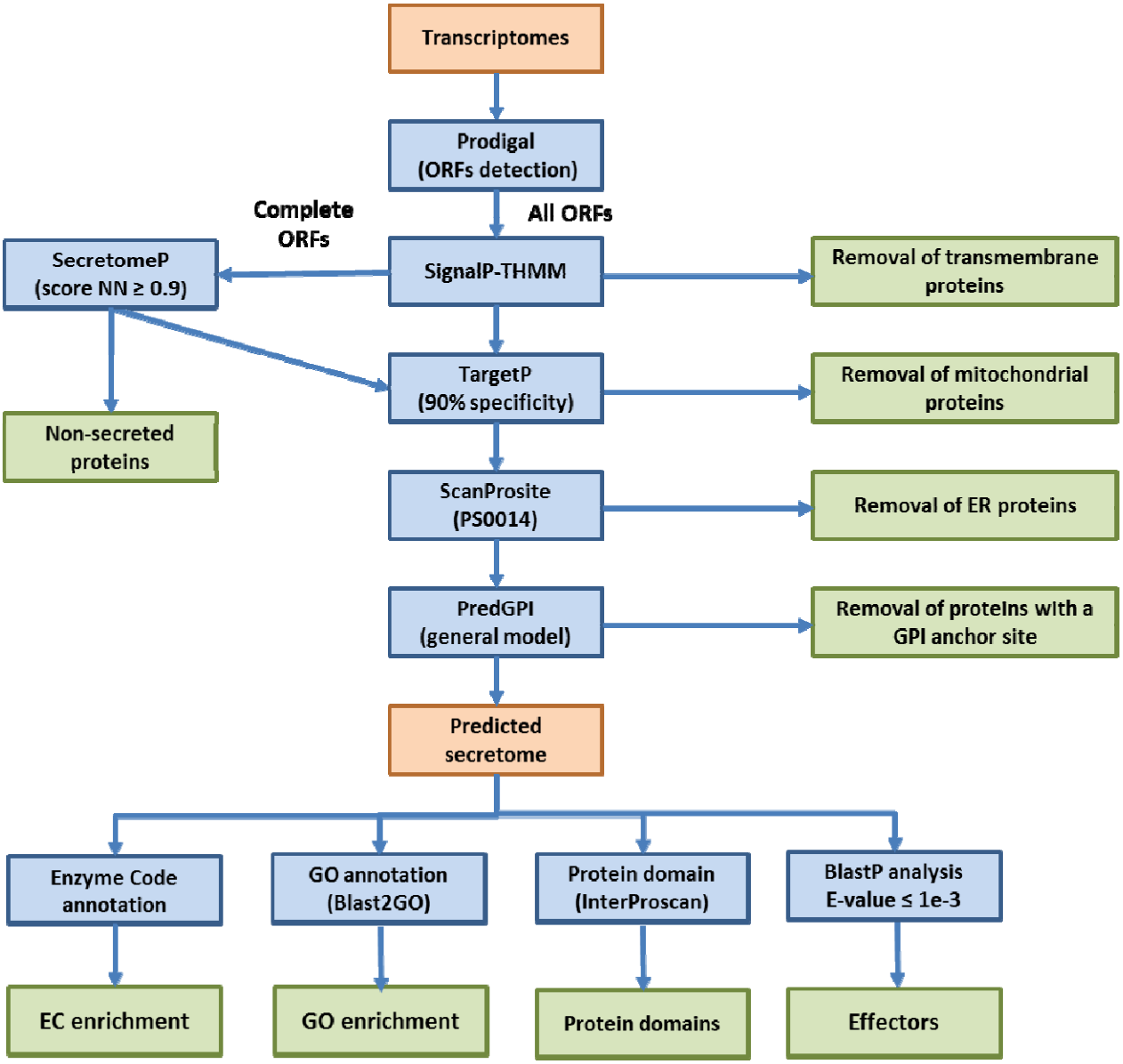

903

904

905 Fig. S2 Mean (± SE) log_2-fold changes of several poplar genes after incubation of I-214 poplar protoplasts
906 with different doses (1, 10, 20 , 40 and 80 µg) of salivary proteins of *Phloeomyzus passerinii* (upper
907 graph) and *Myzus persicae* (lower graph). Two biological replicates were performed for *P. passerinii* and
908 one for *M. persicae*.

909

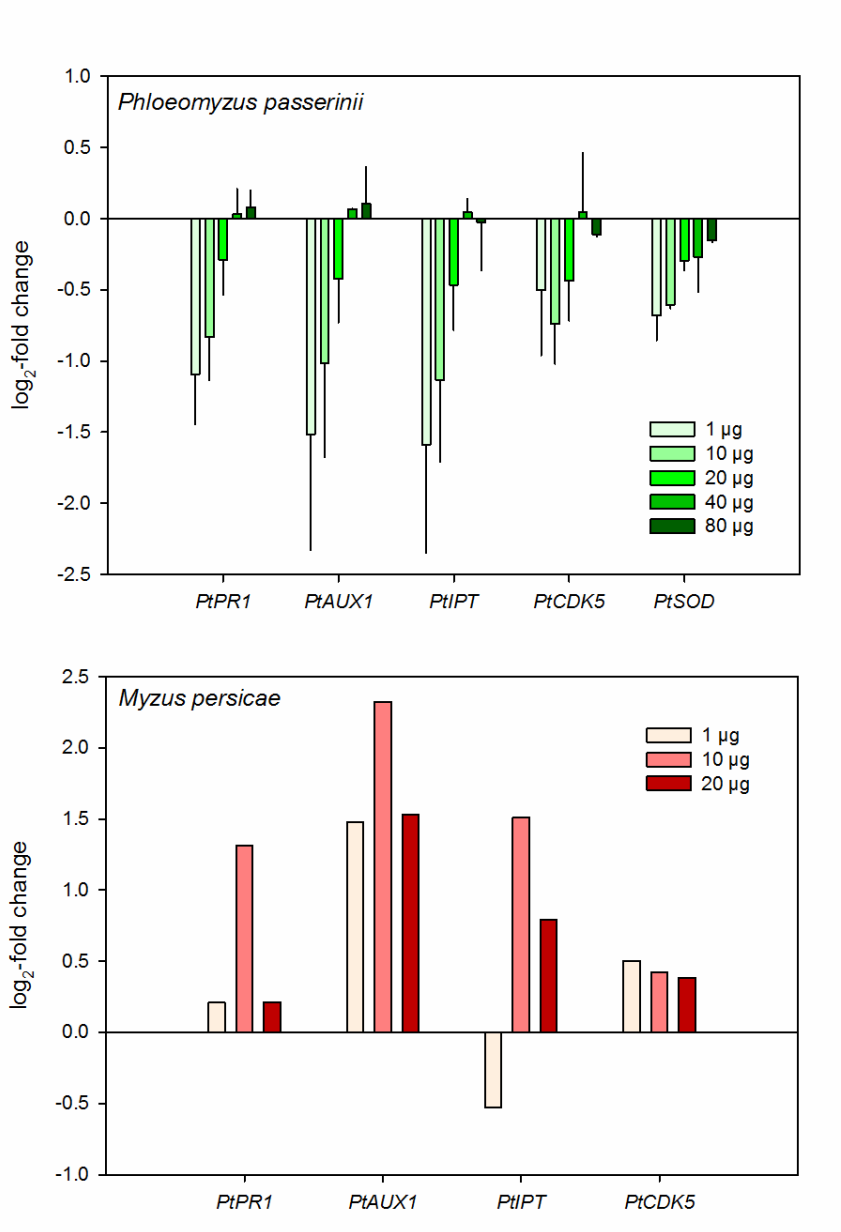

910

911 Fig. S3: FDA assay on poplar protoplasts after 3 h of incubation with salivary proteins of *Phloeomyzus*
912 *passerinii* (A, B) and *Myzus persicae* (C, D). Black bars represent 25 µm. Most protoplasts were
913 fluorescent after treatment, indicating that incubation with salivary proteins of aphids did not affect
914 their survival.

915

916 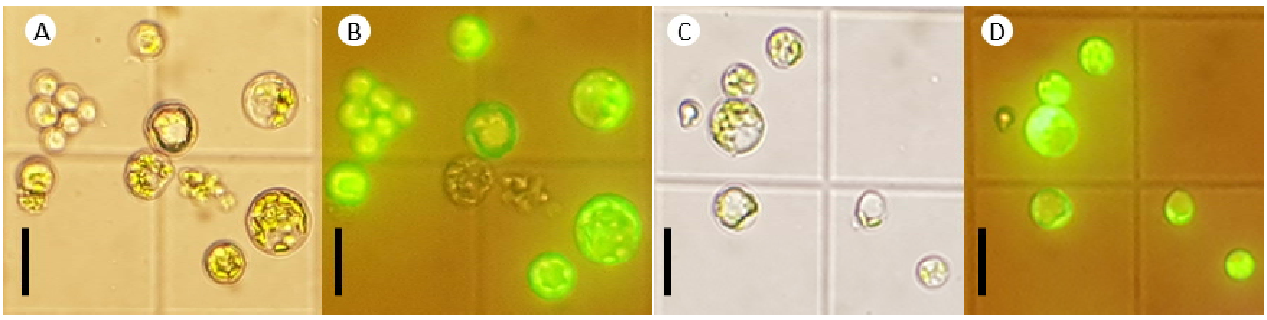

917